Article:
Ibarra-Espinosa, S., de Freitas, E.D., Gaubert, B. et al. (2026) A Century of Vehicular Emissions in Brazil: Unveiling the Impacts of Unique Fuel Mix on Air Quality. Environmental Science and Technology, 60 (6). pp. 4914-4930. ISSN: 0013-936X

https://doi.org/10.1021/acs.est.5c08400

A Century of Vehicular Emissions in Brazil: Unveiling the Impacts of Unique Fuel Mix on Air Quality

Sergio Ibarra-Espinosa[1,2], Edmilson Dias de Freitas[3], Benjamin Gaubert[4], Pablo Lichtig[4,5,6], Karl Ropkins[7], Iara da Silva[3], Guilherme Martins Pereira[3], Daniel Schuch[8], Janaina Nascimento[1,9], Leonardo Hoinaski[10], Leila Droprinchinski Martins[11], Mario Gavidia-Calderón[3], Angel Vara-Vela[12], Taciana Toledo de Almeida Albuquerque[13], Rita Yuri Ynoue[3], Sebastian Diez[14], Zamir Mera[15,16], Alejandro Casallas[17], Fidel Vallejo[18], Valeria Diaz[19], Rizzieri Pedruzzi[20], Rosana Abrutzky[21], Marco A. Franco[3], Nicolas Huneeus[22,23], Hector Jorquera[24,25], Luis Carlos Belalcázar-Cerón[26], Néstor Y. Rojas[26], Maria de Fatima Andrade[3], Louisa Emmons[4], Guy Brasseur[4,27].*

1. Cooperative Institute for Research in Environmental Sciences, University of Colorado-Boulder, Boulder, CO, 80309, United States sergio.ibarraespinosa@colorado.edu.

2. NOAA Global Monitoring Laboratory, Boulder, CO, 80305, United States.

3. Departamento de Ciências Atmosféricas, Instituto de Astronomia, Geofísica e Ciências Atmosféricas, Universidade de São Paulo. São Paulo, 05508-090, Brazil.

4. Atmospheric Chemistry Observations & Modeling Laboratory (ACOM), NSF National Center

for Atmospheric Research (NSF NCAR), Boulder, CO, 80301, United States.

5. Consejo Nacional de Ciencia y Tecnología, Buenos Aires, C1040 AAH, Argentina.

6. Comisión Nacional de Energía Atómica, Buenos Aires, C1429 BNP, Argentina.

7. Institute for Transport Studies, University of Leeds, LS2 9JT, United Kingdom.

8. Civil and Environmental Engineering, Northeastern University, Boston, 02115, United States.

9. NOAA Global Systems Laboratory, Boulder, CO, 80305, United States.

10. Department of Sanitary and Environmental Engineering, Federal University of Santa Catarina (UFSC), Florianopolis, 88040-900, Brazil.

11. Federal University Technology of Paraná (UTFPR), Londrina, Paraná, 86036-700, Brazil.

12. Institute of Physics, University of São Paulo, São Paulo 05508-900, Brazil

13. Departamento de Engenharia Sanitária e Ambiental, Universidade Federal de Minas Gerais. Belo Horizonte, Minas Gerais, 31270-901, Brazil.

14. Centro de Investigación en Tecnologías para la Sociedad, Universidad del Desarrollo, Santiago, 7550000, Chile.

15. Faculty of Applied Sciences, Universidad Técnica del Norte, Ibarra, Ecuador

16. Fundación Alma Verde, Ibarra, Ecuador.

17. Institute of Science and Technology Austria, 3400, Klosterneuburg, Austria.

18. Industrial Engineering, National University of Chimborazo, Riobamba, 060155, Ecuador.

19. Air Quality Monitoring Network, Secretariat of the Environment, Municipality of the Quito Metropolitan District, Quito, 170138, Ecuador.

20. Departamento de Engenharia Sanitária e Ambiental, Faculdade de Engenharia da

Universidade do Estado do Rio de Janeiro, R. 22451-900, Brazil.

21. Grupo de Estudios en Salud Ambiental y Laboral, Universidad Nacional de Avellaneda, Buenos Aires, B1870, Argentina.

22. Center for Climate and Resilience Research (CR)2, Santiago, 8320000, Chile.

22. Department of Geophysics, Universidad de Chile, Santiago, 8320000, Chile.

24. Departamento de Ingeniería Química y Bioprocesos, Pontificia Universidad Católica de Chile, Avda. Vicuña Mackenna 4860, Santiago, 7820436, Chile.

25. Center for Sustainable Urban Development (CEDEUS), Los Navegantes, Providencia, 1963, Santiago, 7520246, Chile.

26. Facultad de Ingeniería, Departamento de Ingeniería Química y Ambiental, Universidad Nacional de Colombia. Bogotá, Colombia.

27. Max Planck Institute for Meteorology, Hamburg, 20146, Germany.

KEYWORDS Brazil, vehicular, emissions, inventory, VEIN, MUSICA, air pollution, biofuels, long-term trends, SSP

ABSTRACT

Global emission inventories often fail to capture the complexities of vehicular pollution in regions with unique fuel mixes, such as Brazil's extensive biofuel use, leading to significant uncertainties in atmospheric modeling. This study presents a century-long (1960–2100)

bottom-up vehicular emission inventory for Brazil, leveraging locally-derived emission factors. Our estimates reveal substantial discrepancies in magnitude, timing, and speciation of non-CO_2 pollutants (CO, NMHC, $PM_{2.5}$) compared to leading global inventories (EDGAR, CEDS, CAMS), highlighting critical inaccuracies in widely used datasets. More critically, future projections under Shared Socioeconomic Pathways (SSPs) uncover a novel positive feedback mechanism: rising temperatures significantly enhance vehicular evaporative non-methane hydrocarbon (NMHC) emissions. This temperature-dependent increase and subsequent NMHC oxidation to CO_2 suggest an overlooked pathway that could amplify climate warming and air pollution globally, particularly after a breakpoint around 2050 ($p<0.05$). While historical emissions peaked in the 1990s-2000s, non-exhaust PM becomes increasingly important. Air quality simulations using our inventory in the MUSICA model show good regional $PM_{2.5}$ agreement but highlight challenges in resolving local primary pollutant peaks. This comprehensive inventory provides crucial data for Brazil and uncovers globally relevant climate-chemistry interactions, urging a re-evaluation of regional specificities in global emission assessments.

SYNOPSIS

This research provides a comprehensive vehicular emission inventory for Brazil, crucial for understanding air quality and climate interactions, especially concerning biofuel use and temperature-driven evaporative emissions.

1. INTRODUCTION

Road transportation is a major source of air pollutants and greenhouse gases. In 2023, it accounted for 21% of global anthropogenic CO_2 emissions[1], but this share rises to 45% in Brazil. The impact of ground transportation was evident during COVID-19 lockdowns, when significant reductions in transport-related air pollutants were observed both locally[2] and globally[3,4]. Despite its importance, there is a lack of long-term studies on emissions trends and their impact on air quality in South America.

Vehicular emissions inventories in South America have focused mostly at the city level, with some applications at the country level. In Chile an inventory[5] developed covering 1990-2020 at 0.01 degree spatial resolution and with an annual temporal resolution. The long-term trend shows continuous growth of CO_2, a peak of nitrogen oxides (NO_X) and $PM_{2.5}$ in 2007, and a peak of carbon monoxide (CO) in 1996 following a steady decrease. In a similar study, an inventory[6] of Colombian transportation emissions for the same period and resolution as the Chilean one[5]. Emission peaks differed between Chile and Colombia: black carbon (BC), CO, NO_X, and $PM_{2.5}$ peaked in 1996, while greenhouse gases such as methane (CH_4) and CO_2 showed continuous growth throughout the period.

Brazil, one of the largest countries in the world, has a population of over 200 million and is one of the countries with the highest consumption of biofuels, where gasoline contains 27% ethanol and diesel 7% biodiesel[7]. During the decade of 1970, Brazil planned an effort to stop the dependency on imported oil with the design of the Proalcool program, which resulted in the development of a car that consumed ethanol instead of gasoline[8]. The blending of ethanol into gasoline began with the Proálcool policy in 1975. Instituted by the military government of Brazil,

the program was a response to the oil crisis of that period. In the meantime, the ethanol content in gasoline ranged from 10% to 22%. Later in 2003, there was the introduction of the flex engine, with the capability to consume any ratio of gasoline and ethanol, as long as the mixture has a composition of 27% ethanol[9]. More recently, by 2024, 76% of the Brazilian fleet consisted of flex-fuel vehicles (more than in any other country), contributing to higher ethanol combustion emissions, and where its atmospheric impacts remain unclear.

In Brazil, an inventory was developed for 2013–2019 at 0.05° spatial resolution, providing hourly emissions with improved spatial detail compared to global inventories[10]. In Brazil, the Ministry of Environment[11] published a national vehicular emissions inventory covering 1980-2009, with projections for 2020. In Argentina, a high-resolution national inventory was published covering 1995-2020[12]. An inventory[13] quantified air pollutant emissions from ground transport in Lima, Peru, by using the US EPA's Motor Vehicle Emission Simulator (MOVES). Other studies in Latin America also investigated air pollution[14,15,16]. The implication is that these studies cover a short amount of period or a limited geographical area. Furthermore, while there are while city-level inventories exist for Latin America (e.g., Santiago, Bogota, São Paulo), there is a distinct lack of long-term, national-level bottom-up inventories that account for the transition of technologies and unique fuel policies over decades.

Building on previous studies and aiming to address the aforementioned gaps, this study improves understanding of long-term vehicular emissions in Brazil by developing a monthly, multi-pollutant inventory spanning from 1960 to 2100. The historical component enables the

analysis of trends driven by key policy interventions and technological shifts, including the implementation of Brazil's biofuel programs. To this end, fuel consumption was reconstructed for 1960-1980 and projected for 2020-2100. We also evaluated the influence of projected temperatures under Shared Socioeconomic Pathways (SSP) to account for the variability of evaporative emissions. Brazilian emissions were calculated using the Vehicular Emissions INventory model (VEIN), an R package with Fortran subroutines[17,18]. To assess the impact of our inventory on air quality simulations and to facilitate its indirect evaluation, we integrated VEIN with the global Copernicus Atmosphere Monitoring Service (CAMS) Global Anthropogenic Inventory version 6.2 (CAMS-GLOB-ANT v6.2)[19] and performed simulations for 2019 using the Multi-Scale Infrastructure for Chemistry Modeling (MUSICA) modeling framework[20]. The performance of the air quality simulation was evaluated against surface air quality observations.

2. DATA AND METHODS

Emissions inventories for road transportation are estimated considering fleet characteristics, mileage, emission factors, and environmental conditions for a specific period[17]. A general formula for estimating emissions is presented in Equation 1:

*Equation 1 Emissions = Activity * Emission Factors*

Where:

- Emissions represent the total mass of a specific pollutant emitted.

- Activity denotes the activity data. For road transport, this is often the total distance traveled by a defined category of vehicles (e.g., vehicle-kilometers, VKT), but it can also be the total fuel consumed by that category.
- Emission Factors represent the mass of a pollutant emitted per unit of activity (e.g., grams per kilometer if activity is VKT, or grams per liter if activity is based on fuel consumption).

Emission Factors are highly specific and vary depending on numerous parameters. These include vehicle type (e.g., passenger car, heavy-duty truck), engine technology, fuel type and composition (e.g., gasoline (G), diesel (D), ethanol (E) content; as in Brazilian gasoline contains 27% ethanol, and diesel blends contain about 7% biodiesel), vehicle maintenance, and operating conditions (such as speed, road grade, and ambient temperature). The units of the total emissions are determined by the units chosen for Activity and Emission Factors. For instance, if Activity is expressed in vehicle-kilometers (km) and Emission Factors in grams per vehicle-kilometer (g/km), then Emissions will be in grams (g). This detailed characterization of emission factors, particularly their fuel specificity, is crucial for assessing the impact of policies such as biofuel programs.

For this study, calculations were performed using the Vehicular Emissions INventory (VEIN) model[17]. VEIN implements this emission estimation framework by utilizing a comprehensive database of emission factors, which includes data from Europe, Brazil, and China, and it can also interface with other models like the US EPA's MOVES[21]. Importantly, VEIN is capable of balancing distance-based activity data with fuel sales or consumption data. This feature allows

for the adjustment of activity levels and the selection and application of appropriate fuel-specific emission factors (whether they are distance-based or fuel consumption-based), ensuring that emissions are estimated consistently with actual fuel usage patterns and characteristics.

2.1. Activity

The vehicle activity data was obtained from the official emissions inventory for the State of São Paulo[7], and they projected it to the country level as described below. For this study, vehicular emissions are estimated between 1960 and 2100, and we need to project data backward and forward. The available vehicle fleet data ranges between 1979 and 2020 at the time of this study. This dataset includes vehicle type, size, and fuel, as shown in Table S1. To model the fleet evolution, we utilized a logistic growth function (Equation 2), a standard approach in the literature for modeling technology adoption and market penetration[22,23,24]. The logistic curve parameters were fitted to obtain the best agreement between the estimated and observed fleet data. This model assumes a saturation point for the market, reflecting that vehicle ownership and fuel consumption cannot grow exponentially forever and will eventually stabilize as the market matures. The maximum age of a vehicle in circulation for this study is 40 years. However, for the year 1960, we assumed that the oldest vehicle in circulation entered the market in 1939 as a conservative approach. Hence, for the historical reconstruction (1939–1978), where official digitized records are absent, we applied a back-casting technique[25]. Given that the fleet size and fuel consumption in the mid-20th century were significantly lower than current levels, we utilized annual reduction factors to project the curves backward from the first year of reliable data.

Specifically, we applied an annual reduction factor of 0.95 for the vehicle fleet. Then we projected the data by fitting a logistic curve shown in Equation 2:

Equation 2 $$f(x) = \frac{L}{\left(1 + e^{-k(x - x_0)}\right)}$$

Where L is the carrying capacity, k is the growth rate, and x_0 is the x value of the function's midpoint. For this study, x_0 is 35, x is the sequence from 1 to 121, L is the maximum number of vehicles per type and state time increased by 20%, and k is 0.15. These numbers were obtained after rigorous tests that resulted in the best agreement with fleet data. Registration of pure ethanol vehicles stopped in 2006. Since the introduction of flex engines, gasoline engine use has decreased over time. Then, to project gasoline engines, we assumed a flat rate of vehicles with the last value of 2020 onwards. After projecting the fleet, we applied a survival function by type of vehicle to obtain the circulating fleet[11]. In other words, we took out the vehicles that were not circulating anymore; for instance, scrapped. The projected circulating fleet is for São Paulo state, which represents an initial fleet. The final fleet, representative of each Brazilian state, is obtained by matching the estimation of fuel consumption and data of fuel sales. Once we have the projected fleet, we move to the next and crucial step: fuel consumption.

Data on fuel consumption by state, month, and type of fuel was obtained from the National Agency of Oil in Brazil[26]. The data used for this study consists of monthly fuel consumption by state from 2000 to 2022. The fuel types include G, which contains 27% of ethanol; E; and D, which contains about 7% of biodiesel. In general, ethanol is produced from sugarcane and

biodiesel from soy. Then, the fuel consumption projected in the past assuming a constant rate of 0.9, and into the future also using logistic Equation 2, but with values of 10 and/or 0.15, L is the max number of vehicles per type and state times 95%. The numbers were obtained after different tests to obtain better agreement with the data. The projections were made yearly until 2100, per state and type of fuel. The monthly fuel consumption was used to calculate the percentage of monthly use, which was assumed constant for the period of projections: before 2000, the monthly distribution of 2000; and after 2022, the distribution of 2022.

Once we have the fleet and fuel for the same period and regions, we estimate the consumer-adjusted fleet, which is the fleet that matches the fuel consumption by each state and year. The process consists of running VEIN to estimate fuel consumption to compare with fuel consumption sales. Then, we calculate the ratio between modelled and actual fuel consumption, using this ratio to correct the initial estimated number of vehicles. This approach assumes that on average, the number of distances is the same for each type of vehicle, varying by age of use. Mileage estimates were based on odometer readings from Brazil[27]. The resulting fleet estimates produce fuel consumption values that closely match recorded fuel sales, with a consumption-to-sales ratio approximately equal to one. This consistency provides confidence in the accuracy of the fleet model and serves as a basis for estimating vehicular emissions.

While the projection of the fleet and fuel in the past relies on assumptions, the uncertainty it introduces is minimized by our "top-down" constraint method. The most critical parameter in our inventory is the total fuel consumption, which depends on the highly reliable official sales data from the National Agency of Petroleum, Natural Gas and Biofuels[26]. Because fuel consumption

in the 1960s and 1970s represents a small fraction of the totals observed during the peak emission decades (1990s and 2000s), the sensitivity of the total inventory to the specific back-casting factor is low (see Before calculating emissions, however, it is necessary to account for appropriate emission factors. Figure S.39).

2.2. Emission Factors

Emission factors in VEIN are based on the official vehicular emissions inventory for São Paulo[7]. These factors come from dynamometer laboratory tests where vehicles undergo a driving cycle that represents the average trip in the city. However, several studies have shown that these do not represent real-world emission factors produced, for example, by intense instantaneous changes in speed and power[28]. On the other hand, tunnel studies measure air composition inside and outside tunnels simultaneously to calculate emissions factors[29,30]. In São Paulo, Brazil, studies have been conducted to determine which emission factors for light and heavy vehicles from tunnels[31,32,33,34,35]. The authors noted a trend of lower emission factors over time, although still higher than those reported by laboratory studies[7].

Nogueira et al. (2021)[34] and Gavidia-Calderón et al. (2021)[36] respectively found that corrected emissions factors in VEIN performed better with observations than laboratory studies when used to model air quality at a mesoscale with WRF-Chem[37] and at street level with MUNICH[38]. To address the gap between emissions factors measured in real-world and laboratory studies, we used emissions factors adjusted with tunnel measurements[7,34]. The tunnel adjustments resulted in factors for CO and VOC between 2.6 and 4.8, NO_X between 0.8 and 1.3, and particulate matter

between 1.6 and 4.1. The emission factors used in this study are shown in the supplementary material section, Figures S3 and S4.

SO_2 emissions depend on the content of sulfur in fuels, which has been regulated since the early 2000s in Brazil[39]. In 2001, the allowed sulfur content was 3500 ppm, with 2000 ppm in the main cities, which decreased over time. To account for the spatial variation in sulfur, we assumed that São Paulo implemented stricter regulations before other states. The results of the sulfur content used in this study are shown in Figure S5.

Evaporative emission factors were converted to g/km following the approach of Ibarra-Espinosa et al. (2020)[40]. As evaporative emissions depend on temperature, between 1960 and 2022 we used average monthly temperatures in each state capital in Brazil, available at the Brazilian Institute of Meteorology[41]. For the projections between 2023 and 2100, we used the Coupled Model Intercomparison Project (CMIP6) ensemble mean data calculated from all the available models[42] and the Shared Socioeconomic Pathway (SSP) 1.9, 4.5, and 8.5. The temporal temperature variation for the mentioned period is shown in Figure S6. Furthermore, we investigated the positive feedback between the projected temperature and the evaporative emissions by applying the Regression Model with Segmented Relationship(s)[43].

Finally, emission factors from tire, brake and road wear were taken from the European Emissions Guidelines[44]. Moreover, for particulate matter (PM) speciation into BC and Organic Carbon (OC), we used field measurements conducted by Pereira et al. (2023)[35], where PM components and their respective emissions factors were quantified in different tunnels in the city of São Paulo, which represent emissions from both light-duty and heavy-duty vehicles. These EFs were

obtained with tunnel measurements in 2018; thus they were influenced by exhaust and non-exhaust emissions, including road dust resuspension. To avoid interference from this dust source, a correction was performed to use the PM EF data (OC, BC, NO_3^-, SO_4^{2-}, and other $PM_{2.5}$). The chemical composition of road dust collected inside the tunnels (Hetem and Andrade, 2016) was adopted to discount its contribution, considering aluminum oxide (Al2O3) as an exclusive road dust tracer. The ratios of pollutant to Al_2O_3 were used to account for the road dust contribution (Table S2). Then, the percentages of pollutants to non-dust $PM_{2.5}$ were recalculated and incorporated into the "pm2025" speciation module, included in the latest version of the VEIN model[17]

2.3. Emissions

We used the Vehicular Emissions INventory model (VEIN), version v1.2.0, which is an R package with Fortran subroutines[17]. One key characteristic of VEIN is the calibration of fleet activity with fuel sales before estimating emissions. In VEIN, datasets are typically processed as data.table[45], which optimizes handling, and then converted to spatial features[46] to enable efficient geo-mapping. VEIN also employs automatic units management functions from the R package units[47].

For this work, emissions for the years 2018 and 2019 were gridded into surface fluxes with a spatial resolution of 0.1 degree to match CAMS-GLOB-ANT 6.2 global emissions inventory[19]. We provide scripts to grid emissions outputs according to user needs in the URL https://github.com/ibarraespinosa/musica_vein. The process consists of first distributing the emissions into roads, in this case from OpenStreetMap[48], and gridding the fluxes. Map data are

copyrighted by OpenStreetMap contributors and available at https://www.openstreetmap.org[49]. Once the emissions were estimated, we applied a speciation of non-methane hydrocarbons (NMHC) by type of vehicle, fuel, and emissions standard, tuned for Brazil[50]. The list of NMHC species can be seen in Table S3. VEIN includes functions to group NMHC species into chemical mechanisms following Carter (2015)[51]. We used five hydrocarbon speciations, exhaust and evaporative from light-duty gasoline and ethanol vehicles, and only exhaust for all diesel vehicles. Then, the species were grouped into the same species as CAMS.

To construct the emissions input for this study, a hybrid global anthropogenic emissions dataset was created, using CAMS-GLOB-ANT 6.2 as the base inventory. Within Brazil, the CAMS-GLOB-ANT 6.2 emissions were replaced with VEIN estimates for the road transportation sector specifically. Its development relies on integrating foundational inventories EDGAR v5.0[52] for historical data and CEDS to extrapolate emissions forward, ensuring temporal consistency and coverage for recent years required by atmospheric models[53].

2.4. MUSICA model

The Multiscale Infrastructure for Chemistry and Aerosols (MUSICA) is an advanced modeling framework[20] developed by the National Science Foundation National Center for Atmospheric Research (NSF NCAR). MUSICA aims to integrate various scales and processes of atmospheric chemistry and aerosol modeling, with the goal of a more comprehensive understanding of air quality, climate interactions, and related processes. MUSICA uses a variable-resolution grid, enabling finer resolution in regions of interest (e.g., urban areas) while maintaining coarser

resolution elsewhere, thereby combining global, regional, and local-scale processes in a single framework.

Specifically, MUSICA version 0 (hereafter MUSICAv0) is a configuration of the Community Atmosphere Model with chemistry (CAM-chem), a component of the Community Earth System Model (CESM), that uses the spectral element dynamical core presented in Lauritzen et al., (2018). We use the same grid presented and evaluated in Lichtig et al., (2024)[54]. The nominal spatial resolution is approximately 100 km (ne30) with a refinement of about 28km (ne30x4) over South America. Following Lichtig et al., (2024)[54], we use the year 2018 as a spinup for the atmospheric chemistry (CAM-chem) using spinup land and atmospheric initial conditions, and we analyze results for 2019. The gas-phase chemical mechanism is MOZART-TS1.2[55] and the aerosol scheme is the Modal Aerosol Module (MAM4) with volatility basis set (VBS) secondary organic aerosols[56,57]. The meteorological dataset used to nudge wind and temperature conditions comes from Modern-Era Retrospective Analysis for Research and Applications, Version 2 (MERRA-2)[58]. Fire emissions are taken from the Fire INventory from NCAR version 2.5 (FINNv2.5)[59], anthropogenic emissions from CAMS-GLOB-ANTv6.2[19], and the Model of Emissions of Gases and Aerosols from Nature (MEGAN) version 2.1 online in CESM for biogenic emissions[60]. The CAMS-GLOB-ANT 6.2 inventory provides comprehensive global gridded emissions with 0.1°x0.1° spatial resolution for key air pollutants and greenhouse gases across numerous anthropogenic sectors, updated regularly to support atmospheric modeling[19]. MUSICAv0 was run on the derecho supercomputer, at the NSF National Center for Atmospheric Research[61].

For the evaluation of MUSICAv0 we utilized surface station data from South America, primarily downloaded from official government environmental agencies. Specifically, data for Chile were obtained using the R package AtmChile[62]. For Brazil, the R package QualR[63] provided data sites in Rio de Janeiro and São Paulo. Data for Peru was obtained with the R package limaair[64]. Data for Ecuador were accessed via the R package AirEcuador[65]. In the case of Colombia, we use hourly observations from the SISAIRE monitoring network[66], which were quality controlled following Casallas et al., (2024)[67]. For other South American countries, daily resolution data (median, minimum, and maximum) were downloaded directly from https://aqicn.org/. Table S3 in the supplementary material includes the list of stations used in this study, and Figure S30 shows the corresponding map.

3. RESULTS

3.1. Activity

The national projection of fuel consumption is shown in Figure 1. Observed data are represented by filled circles over a gray background, while projections are shown both before and after these observations. Diesel is the most consumed fuel (millions of tons), followed by gasoline and then ethanol. However, there are strong regional and compositional differences. Considering the year 2018, the state with more consumption was São Paulo (SP) with 27%, followed by Minas Gerais (MG) with 11% and Paraná with 9%. The state with the largest ethanol consumption is SP with 51%, followed by MG with 13%, and PR with 8%. Regarding gasoline, the largest consumption is again SP with 22%, then MG with 9%, and Rio Grande do Sul (RS) with 9%. Finally, the

consumption of diesel is dominated by SP with 22%, MG with 12%, and PR with 10%. A table with all state abbreviations is shown in Table S4.

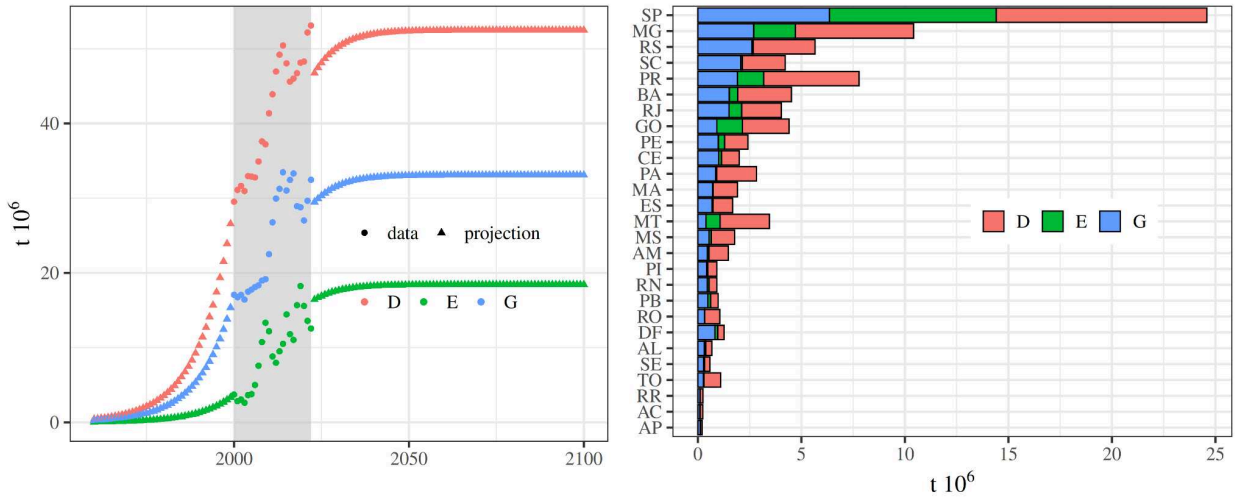

Figure 1. a) Fuel consumption in Brazil from 1960 to 2100 (million t/year) by year, type of fuel, and fuel consumption (data) and their projections, and b) fuel consumption in Brazil in 2018 by state and type of fuel (million t/year). The grey rectangle in panel a) indicates the years with available registry data.

3.2. Emissions estimates

3.2.1. CO_2

Figure 2 presents the estimated trends of total CO_2 and fossil fuel CO_2 ($FFCO_2$) emissions originating from Brazil's road transportation sector for the period 1960-2100. These emissions were calculated using the VEIN model, with results disaggregated by fuel type: Diesel (D),

Ethanol (E), and Gasoline (G). The $FFCO_2$ is derived by excluding the biogenic carbon component associated with the biofuels used. This involved removing CO_2 attributed to the combustion of 100% ethanol fuel, 27% ethanol blended into gasoline, and 8% biodiesel blended into diesel. For comparative purposes, corresponding road transport sector emissions from three global inventories, EDGAR v8.1[1], EDGAR v5.0[52], CEDS v2024_07_08[68], and CAMS-GLOB-ANT v6.2[19] are overlaid as lines in both panels.

A key observation from Figure 2 is the general agreement in historical trends and magnitudes between the VEIN model estimates and the global inventories, particularly EDGAR v8.1 and CEDS v2024_07_08. This consistency is evident for both total CO_2 and, notably, for $FFCO_2$ emissions. Such alignment is expected, as CO_2 emissions are primarily driven by fuel consumption (activity data), which is often more consistently represented across different datasets compared to emission factors for other pollutants. The VEIN estimates, based on national fuel consumption statistics, capture the overall trajectory of Brazil's road transport CO_2 emissions as reflected in major global inventories. While minor variations exist, the overall consistency underscores the robustness of the activity data and modeling approaches for CO_2 from this sector, implying that discrepancies observed for non-CO_2 pollutants between inventories are likely dominated by differences in emission factors. However, discrepancies arise in the emission estimates prior to 1980. Since our projections extend fuel use backward before 2000, and given that literature-based estimates may incorporate more historical data for Brazil, we may be underestimating past emissions during this earlier period.

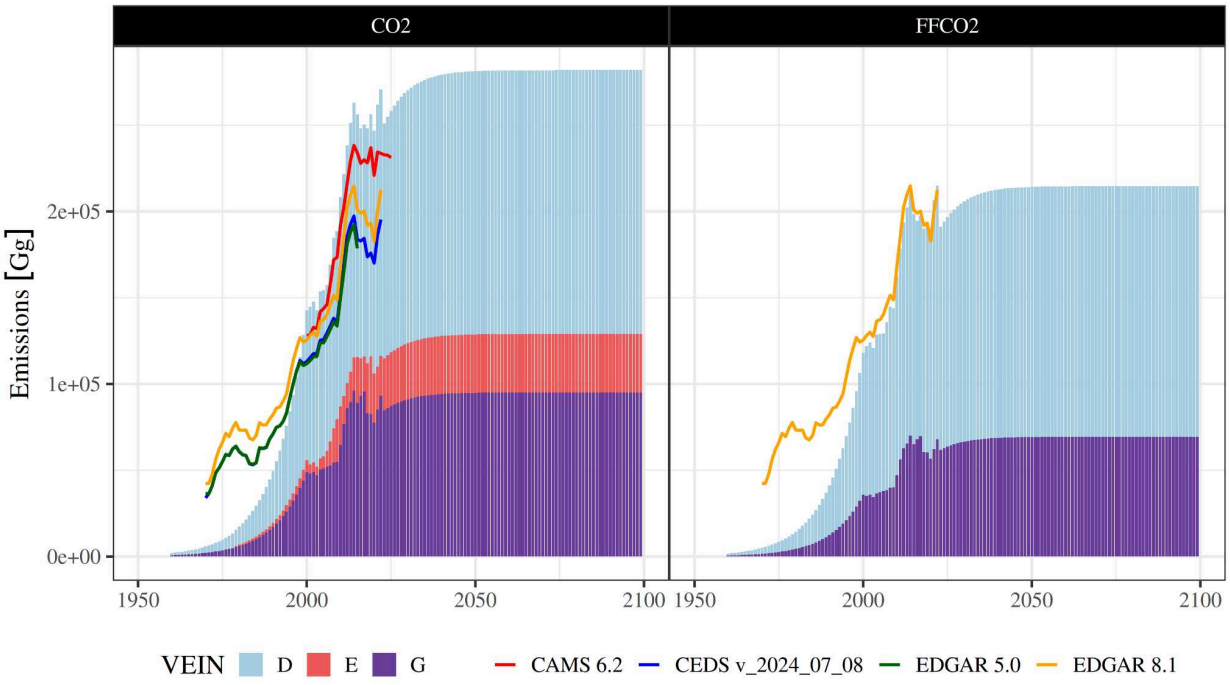

Figure 2. Emissions of CO_2 from the transportation sector in Brazil (1960–2100) by fuel type (left). The figure also includes fossil fuel CO_2 ($FFCO_2$), representing CO_2 emissions, excluding contributions from ethanol and biodiesel (right). Historical emissions from EDGAR v5.0[53], EDGAR v8.1[1], CEDS v2024_07_08[68], and CAMS-GLOB-ANT v6.2[19] are overlaid for validation.

3.2.2. Air pollutants other than CO_2 and NMHC

Figure 3 compares historical (1950-2100, with projections extending based on VEIN) road transportation emissions for Brazil estimated using the VEIN model against four global inventories: CAMS-GLOB-ANT v6.2, EDGAR v5.0, EDGAR v8.1, and CEDS v2024_07_08. The panels display emissions for various key pollutants, including BC, CH_4, CO, Nitrous Oxide (N_2O), Ammonia (NH_3), NO_X, OC, Particulate Matter (PM_{10} and $PM_{2.5}$), and SO_2. NO and NO_2

are estimated separately in VEIN. VEIN estimates are shown as stacked bars representing contributions from Diesel (D), Ethanol (E), and Gasoline (G) fuels, while the global inventories are overlaid as lines. In addition, we investigated the influence of the type of vehicle and fuel on each pollutant. For instance, 80% of CO is emitted by vehicles consuming gasoline or ethanol, while diesel vehicles emit 91% of NO_X and 85% of BC, as shown in Figure S7.

The VEIN emission estimates show distinct temporal patterns influenced by fuel consumption, fleet characteristics, emission factors derived from real-world measurements, and the implementation sequence of Brazilian vehicle emission standards (PROCONVE for light- and heavy-duty vehicles; PROMOT for motorcycles). Peak emissions for most pollutants occurred between 1990 and 2015: CO peaked in 1993 (8553 Gg y^{-1}), NO_X and CH_4 in 2000 (1467 and 122 Gg y^{-1}, respectively), BC, OC, $PM_{2.5}$, and PM_{10} in 2001 (53, 38, 106, 110 Gg y^{-1}, respectively), SO_2 in 2008 (210 Gg y^{-1}), and NH_3 in 2014 (41 Gg y^{-1}). Under a business-as-usual scenario reflecting projected fleet and fuel consumption growth, N2O emissions are expected to continue rising, reaching a maximum of approximately 22 Gg y^{-1} by 2100.

Comparing VEIN with the global inventories reveals substantial differences for most non-CO2 pollutants, including BC and OC. VEIN frequently estimates different peak emission magnitudes and timings compared to CAMS-GLOB-ANT v6.2, EDGAR 8.1 and 5.0, and CEDS v2024_07_08. For instance, while EDGAR and CEDS v2024_07_08 often show peaks around 2000 for many species (e.g., BC, OC, PM), VEIN's peak values can occur earlier (e.g., CO) or later (e.g., NO_X, CH_4) and generally reach higher magnitudes. CAMS often displays significantly later peaks (e.g., ~2010-2015 for BC, OC, and NO_X). Furthermore, it is clear how

CAMS-GLOB-ANT v6.2 emissions agree with EDGAR 5.0, the basis emissions model for CAMS. Then, it is possible that a newer version of CAMS-GLOB-ANT v6.2 will agree with EDGAR 8.1.

These discrepancies across the range of non-CO_2 species strongly suggest that variations in emission factors are the primary driver of differences between the regional VEIN model and the global inventories. While CO_2 emissions are largely constrained by fuel consumption data (activity data), the emission rates of other pollutants are highly sensitive to assumptions about vehicle technology, after-treatment systems, operating conditions, and fuel properties, which likely differ between VEIN's bottom-up, potentially locally tuned approach and the more generalized methodologies used in global datasets. Furthermore, analysis indicates a growing future significance of non-exhaust particulate matter from tire and brake wear (included in PM_{10}/$PM_{2.5}$ totals), which lack specific control technologies in Brazil. Specifically, in 2032 is the first year where wear emissions will be higher than exhaust, with a factor of 1.04. After that, this factor will grow up to, and stabilize at 1.4 in 2048. Because non-exhaust emissions have documented deleterious effects on both human health and ecosystems, it is key that future environmental policies account for and mitigate these sources to ensure the long-term protection of the population and the environment[69].

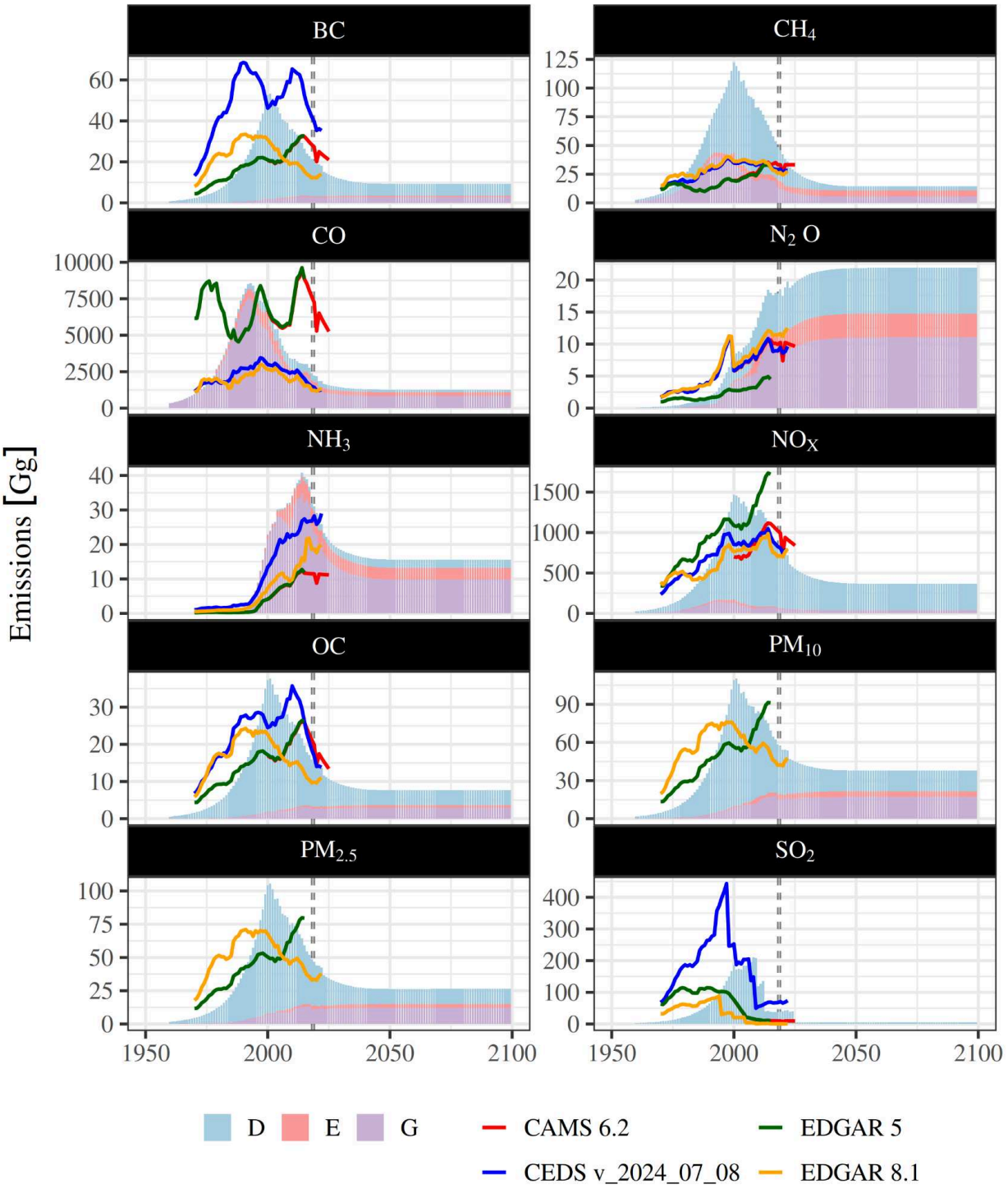
BC
CH4
CO
N2 O
NH3
NOX
OC
PM10
PM2.5
SO2
Emissions [Gg]
1950
2000
2050
2100
D
E
G
CAMS 6.2
EDGAR 5
CEDS v_2024_07_08
EDGAR 8.1

Figure 3. Emissions trends for BC, CH_4, CO, N_2O, NH_3, NO_X, OC, PM_{10}, $PM_{2.5}$, and SO_2 from the transportation sector in Brazil from 1960 to 2100, as modeled using VEIN. The results are categorized by fuel type: diesel (D), ethanol (E), and gasoline (G). Historical emissions from EDGAR v5.0[53], EDGAR v8.1[1], CEDS v2024_07_08[68], and CAMS-GLOB-ANT v6.2[19] are overlaid for validation. The vertical lines represent the 2018 and 2019 years used in the MUSICA air quality simulation.

3.2.3. Exhaust and evaporative NMHC

Figure 4 presents estimated NMHC emissions from Brazil's road transportation sector. The first panel shows the historical trend of total NMHC emissions (exhaust + evaporative) calculated using the VEIN model (VEIN Historic), compared to four global inventories: EDGAR v5.0, EDGAR v8.1, CEDS v2024_07_08, and CAMS-GLOB-ANT v6.2. The VEIN projected curve includes future evaporative NMHC emissions (2020–2100) under three SSP scenarios, representing approximate radiative forcing targets of 1.9, 4.5, and 8.5 W m^{-2} by 2100. Since the projection applies only to evaporative emissions (which contribute a smaller share compared to exhaust), the projected values are similar and closely aligned; hence, they are plotted with the same color. However, they are not identical.

The historical comparison reveals notable differences in peak magnitude and timing. VEIN estimates a peak in 1993, significantly higher than EDGAR v8.1 and CEDS v2024_07_08, which both peak around 2000. Nevertheless, the overall trend (a rise followed by a decline) is consistent across VEIN, EDGAR v8.1, and CEDS. In tandem, CAMS-GLOB-ANT v6.2 and EDGAR v5.0 show a later and higher peak around 2010–2015. These discrepancies underscore the sensitivity

of NMHC estimates to differences in methodology and input data. As with other non-CO_2 pollutants, the magnitude of these differences likely stems from the emission factors used: VEIN relies on region-specific, real-world measurements, while global inventories tend to apply more generalized values.

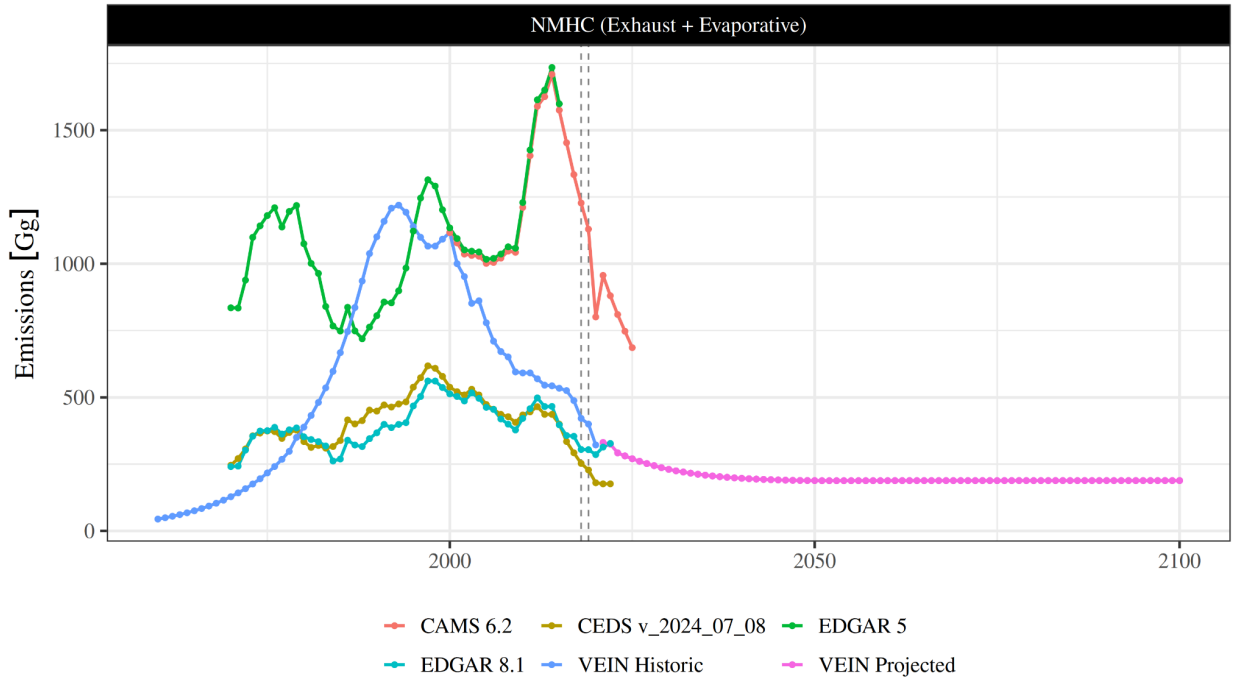

Figure 4. Emissions of non-methane hydrocarbons (NMHC). The lines represent the Historical emissions from EDGAR v5.0[53], EDGAR v8.1[1], CEDS v2024_07_08[68], and CAMS-GLOB-ANT v6.2[19] are overlaid for validation. The magenta lines (three lines) show future projections based on Shared Socioeconomic Pathways (SSP1-1.9, SSP4-4.5, SSP5-8.5). They were colored with the same color because the values are very close, avoiding the unnecessary inclusion of more colors in a longer legend. The vertical lines represent the 2018 and 2019 years used in the MUSICA air quality simulation. Distinct evaporative emissions are shown in Figure 5.

3.2.4. Positive Feedback

Evaporative emissions projected in the future are shown in the first panel of Figure 5. Here we see that starting in the 2050s, the spread of the values increases with an increasing difference between emissions based on temperature extremes. To further investigate the influence of temperature on projected evaporative NMHC emissions, a segmented regression analysis was performed using established methods[43], as shown in the right panel. The VEIN projected estimation exhibits a sharp decline from 2020 until approximately 2050 as a result of the technologies associated with the emissions controls and turnover fleet. Interestingly, after 2050, the projections show a slight increase and a growing divergence between the scenarios. This suggests a potential temperature influence on evaporative processes becoming more apparent in the long term under warmer scenarios (like the 8.5 W m^{-2} pathway), although the overall magnitude of evaporative emissions remains low in this future period compared to historical total NMHC levels. This projected increase in evaporative emissions contrasts with the expected continued decline in exhaust NMHC emissions due to stricter vehicle standards.

The analysis focused on the period after the initial sharp decline in evaporative emissions (post-2020, as shown previously) revealed a statistically significant "hockey-stick" relationship between projected temperature pathways and evaporative NMHC emissions. A breakpoint was identified around the year 2053, after which evaporative emissions exhibit a statistically significant increasing trend. This increase is positively correlated with temperature and is notably more pronounced under the warmer SSP2-4.5 and SSP5-8.5 scenarios. Given that atmospheric

oxidation of NMHC contributes to CO_2 formation, this temperature-driven increase in evaporative emissions suggests a potential positive feedback mechanism.

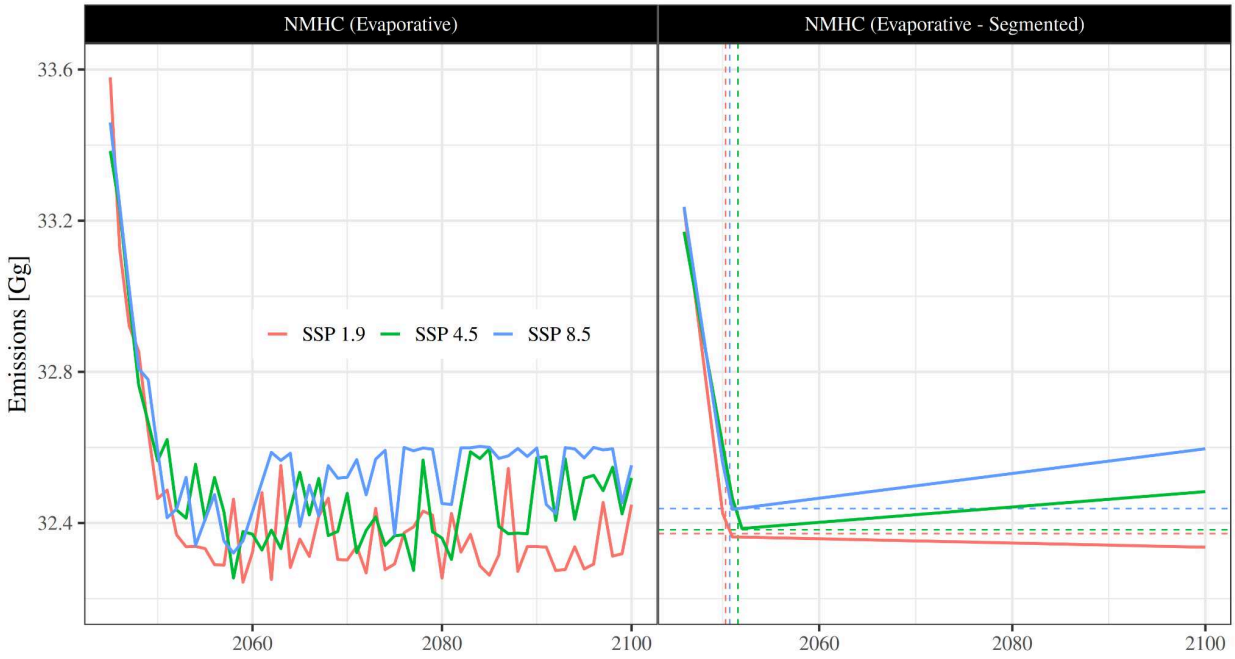

Figure 5. Evaporative emissions of non-methane hydrocarbons (NMHC) projections based on Shared Socioeconomic Pathways (SSP 1.9, SSP 4.5, SSP 8.5) (left) and segmented regressions (right) (Gg).

3.2.5. Emission maps

Figure 6 presents a spatial comparison of annual average road transport emissions for selected pollutants over Brazil, contrasting estimates from the regional VEIN model with the global CAMS-GLOB-ANT v6.2 inventory for the year 2018. The figure displays results for CO in panel

a, NOX in panel b, and Alcohols in panel c. For each pollutant, maps depict the spatial distribution estimated by VEIN, CAMS, and the absolute difference between them (VEIN - CAMS-GLOB-ANT v6.2). We selected CO because it mostly represents emissions from 4-stroke engines, NOX for diesel engines, and alcohols due to their unique alcohol presence in Brazilian fuels. The comparisons reveal distinct patterns for each species. For both CO and NO_x, the CAMS-GLOB-ANT v6.2 inventory generally estimates higher annual average emissions than VEIN, particularly in southeastern Brazil, as shown with negative values (blue shading) in the difference maps for these areas, which are also depicted in Figure 3. While both models capture the general location of major source areas, CAMS tends to show higher emissions in capitals, while VEIN shows more differences across states.

Furthermore, VEIN appears to capture emission patterns along major regional highway corridors compared to the more diffuse patterns in CAMS, possibly due to incorporating more detailed or updated road network data (e.g., from OpenStreetMap). These differences likely reflect variations in spatial proxies and the representation of fleet characteristics (especially relevant for NO_X from diesel vehicles). In contrast, the comparison for Alcohols (Figure 6) shows a different pattern where spatial allocation is key. VEIN estimates are significantly higher than CAMS-GLOB-ANT v6.2 in São Paulo state (strong positive differences, red shading), while CAMS emissions are more diffuse and sometimes higher in surrounding, lower-emission areas. This spatial pattern in VEIN aligns well with known activity, as the São Paulo state region accounts for the highest ethanol consumption within Brazil's vehicle fleet.

Therefore, while total values from CAMS might be comparable or higher, VEIN's spatial allocation appears more realistic for this biofuel-related emission, and this difference in spatial representation is particularly pronounced for alcohols compared to the other pollutants examined. This highlights the critical impact of specific biofuel representation and detailed activity data allocation in the regional VEIN model compared to the more generalized approach of the global CAMS-GLOB-ANT v6.2 inventory. These examples underscore that differences between regional and global emission estimates vary substantially by pollutant in terms of magnitude, spatial allocation, and even the direction of the difference. Furthermore, a comparison of domain-averaged monthly emission cycles revealed distinct differences in seasonality between VEIN and CAMS-GLOB-ANT v6.2 for several key species, with VEIN generally exhibiting more pronounced monthly variations (see Figure S29). These significant discrepancies in both magnitude and spatial distribution have important implications for accurately modeling regional air quality impacts in Brazil. This also reflects the importance of the development of local emissions inventories. The spatial maps for the other pollutants are shown in the supplementary material.

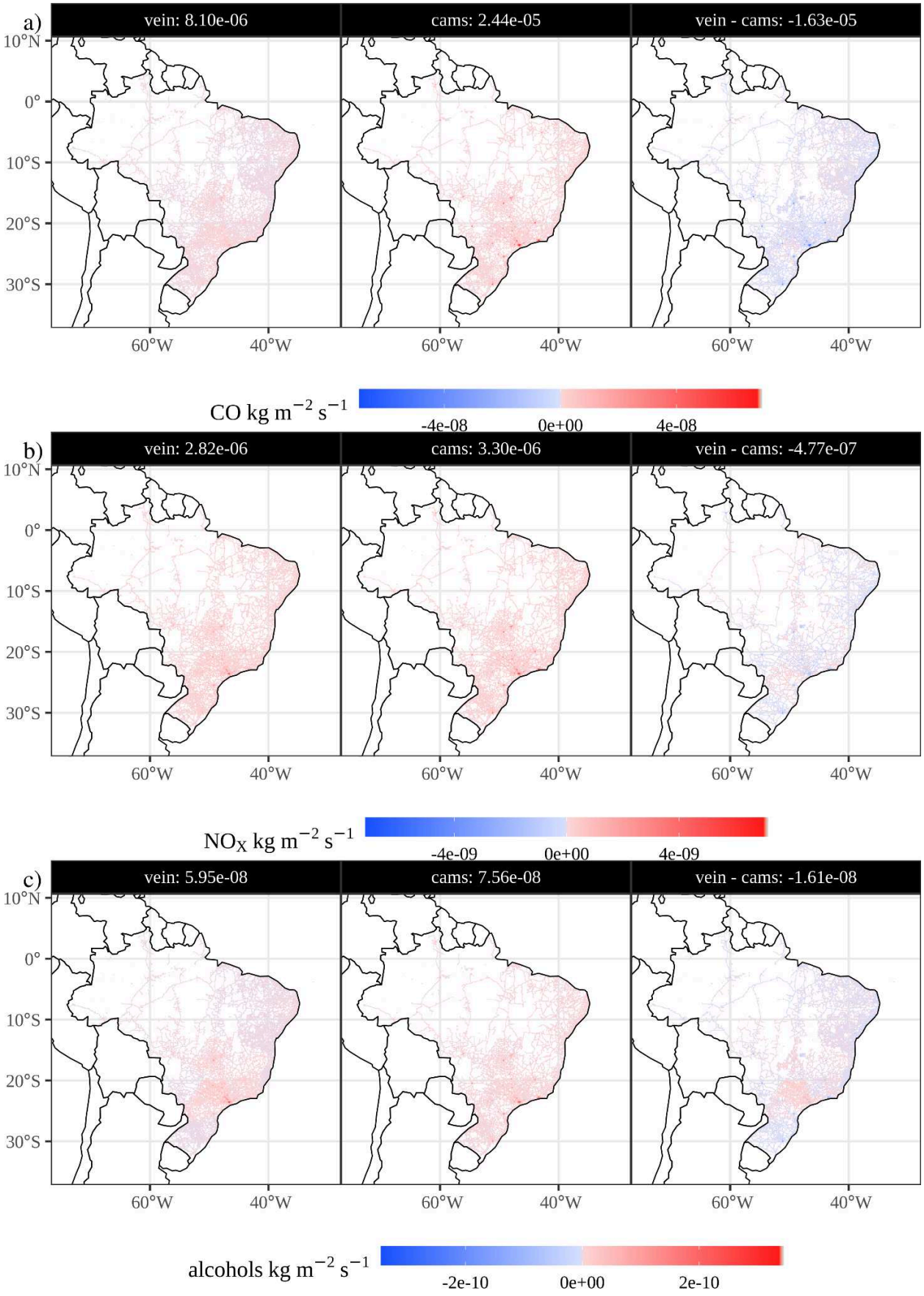
a)
vein: 8.10e-06
cams: 2.44e-05
vein - cams: -1.63e-05
10°N
0°
10°S
20°S
30°S
60°W
40°W
CO kg m^{-2} s^{-1}
-4e-08
0e+00
4e-08
b)
vein: 2.82e-06
cams: 3.30e-06
vein - cams: -4.77e-07
NO$_X$ kg m^{-2} s^{-1}
-4e-09
0e+00
4e-09
c)
vein: 5.95e-08
cams: 7.56e-08
vein - cams: -1.61e-08
alcohols kg m^{-2} s^{-1}
-2e-10
0e+00
2e-10

Figure 6. Emissions fluxes of CO (a), NOX (b), and alcohols (c) from VEIN and CAMS-GLOB-ANT v6.2 (denoted as cams) including the differences, 0.1ºx0.1º kg m^{-2} s^{-1} for the year 2018.

3.3. Air quality in Brazil

The air quality evaluation indicated that the strongest agreement between MUSICA and observations was generally found in Brazil (specifically in São Paulo and Rio Grande do Sul states) and Chile. Figure S32 shows the correlation coefficients between MUSICA simulations and observations from the available stations, calculated using the R package eva3dm[70]. Likewise, Figure S33 shows the normalized mean bias as a percentage. However, considerable variability exists in the results; correlations tend to be weaker in regions with more complex terrain, city size, and other parameters. In addition, Pachon et al. (2024)[71] show that the size of the city is also an important factor to model air quality. It is important to consider that global emissions inventories often have limitations in South America[17,72]. Consequently, local efforts have been undertaken to develop regional emissions inventories for South America[73,74]. Furthermore, the analysis indicated that the use of data from the AQICN website is not recommended due to the lower correlations observed when compared with data from official state networks.

3.3.1. CO

The air quality evaluation demonstrated generally good agreement between the MUSICA simulations and station-level observations (Figure 7). We employed a hierarchical approach wherein observations from state networks, such as CETESB (Brazil) and SINCA (Chile), were

prioritized for selection. Data obtained from the AQICN webpage were generally found to be less reliable, exhibiting discrepancies when compared to state observations available for the same cities. In this section, we present comparisons specifically with stations in Brazil; the comparison with other countries is provided in the supplementary material. The comparison between MUSICA using only CAMS emissions and MUSICA using CAMS combined with VEIN emissions showed very similar results for most pollutant concentrations, with the notable exception of CO, for which MUSICA-CAMS yielded higher concentration values, although the difference is small. This difference is attributed to the higher values present in the CAMS emissions inventories, as previously discussed.

Figure 7 shows the monthly mean CO concentrations (in ppb). The red line represents simulations from MUSICA-CAMS, the green line represents MUSICA-CAMS combined with VEIN emissions, the blue line corresponds to observations from CETESB (the environmental agency of São Paulo state), and the purple line shows observations from FEPAM (the environmental agency of Rio Grande do Sul state). The overall average CO concentration across these stations is 222.9 ppb for MUSICA-CAMS and 163.9 ppb for MUSICA-CAMS+VEIN. The shaded area represents half of the standard deviation (0.5σ). Given the longer operational periods and thus higher reliability of CETESB observations, the y-axis scale for the comparison was limited between 0 and the maximum observed values from CETESB. This scaling excluded some observations with excessively high values, such as those recorded at the Guaiba Parque station. We also observe that simulations in Sao Paulo capture a seasonal peak during the dry period (June-August), which is not reproduced by the MUSICA simulation, likely due to its spatial

resolution of ~25 km. This is further supported by the greater agreement found at more regional or intercity stations, such as Triunfo Polo, compared to street-level stations like Pinheiros. A comprehensive list of stations and their coordinates can be found in Table S5, and a map in Figure S32. The station Guaiba Parque, located in south Brazil, has surprisingly high values. We contacted the environmental agency to double-check the units and location of the station. Then, more research is needed to investigate this station, since it may be impacted by a local source not available in current inventories.

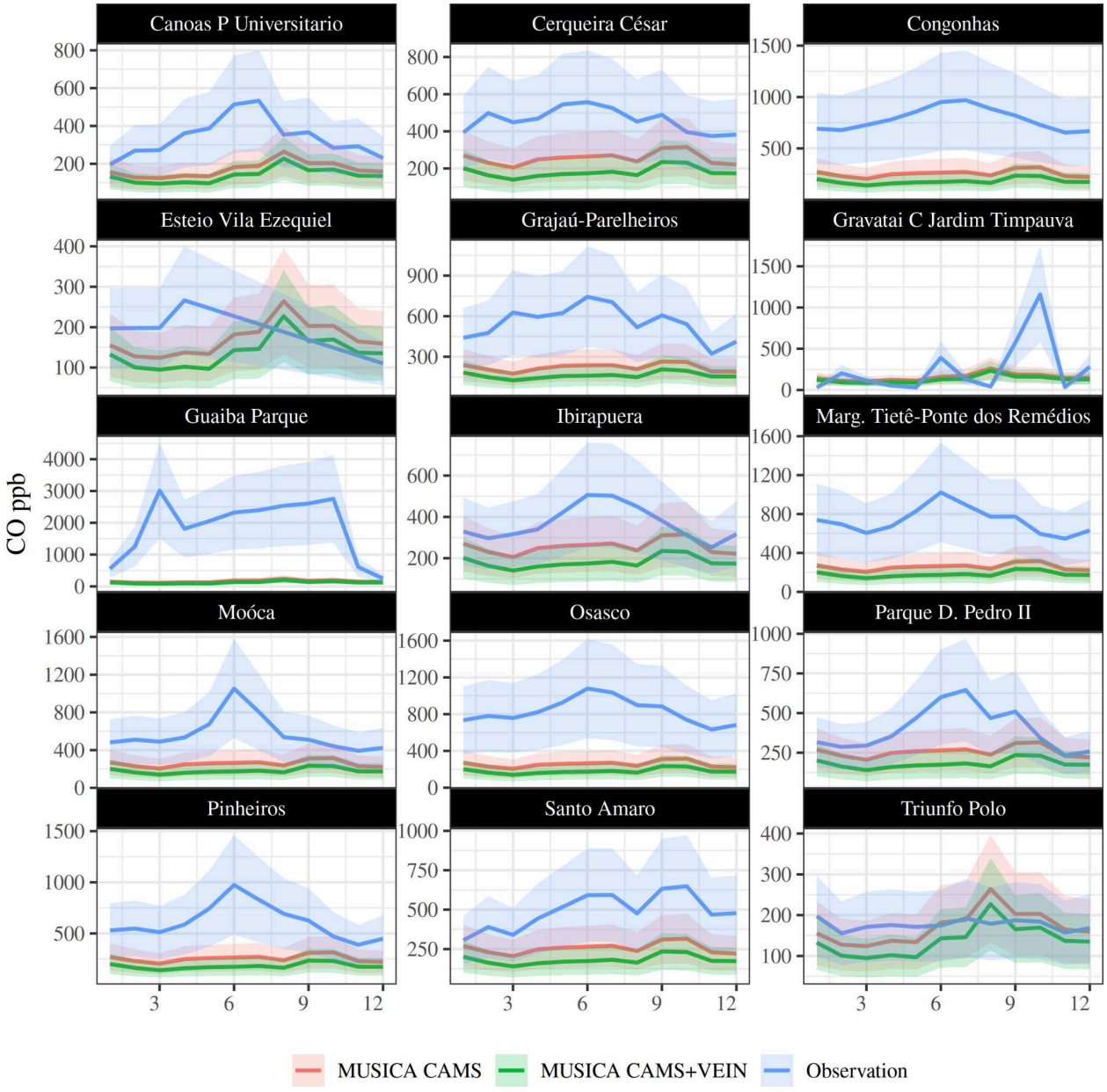

Figure 7. Comparison between MUSICA CAMS, MUSICA-CAMS+VEIN, observations from the environmental protection agency in Brazil São Paulo CETESB (https://cetesb.sp.gov.br/ar/) and Rio Grande do Sul (https://www.fepam.rs.gov.br/ar) as monthly mean of CO (in ppb) for 2019.

The differences observed in the time series extend spatially, as shown in Figure 8, where we see annual differences in CO concentrations between the MUSICA-CAMS and MUSICA-CAMS+VEIN simulations. More significant differences are indeed observed in Southeast Brazil, a region characterized by a larger vehicle fleet and fuel consumption. A small increment in CO concentrations is also visible in Central-West Brazil, specifically in the state of Acre. The availability of a detailed spatial emissions inventory like VEIN allows for a clearer representation of spatial differences among air quality model scenarios.

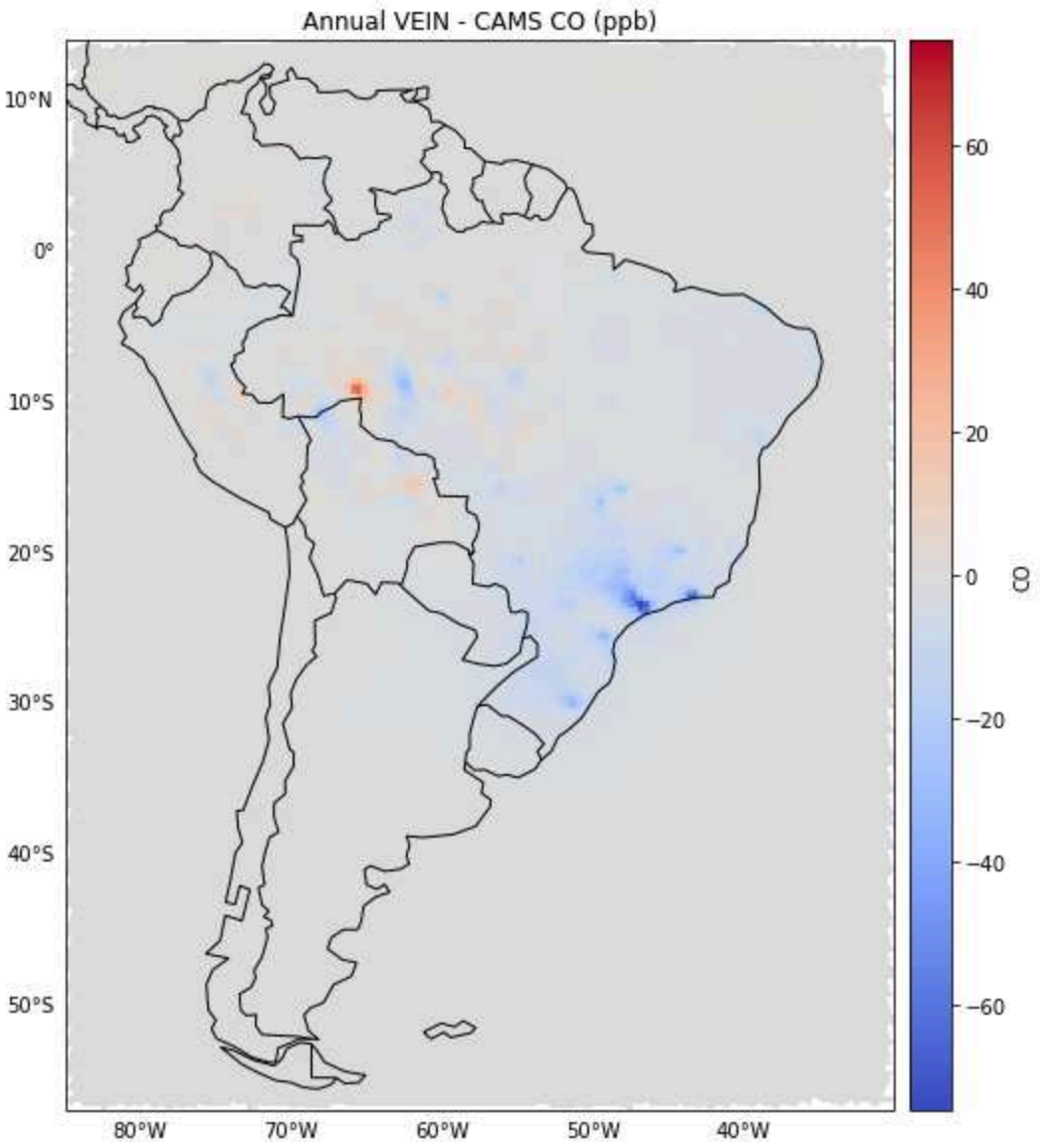

Figure 8. Annual difference between MUSICA-CAMS and MUSICA-CAMS+VEIN CO (in ppb) for the year 2019.

3.3.2. O_3

For the case of O_3 and the rest of the analyzed pollutants, there was no clear difference between the MUSICA-CAMS and MUSICA-CAMS+VEIN simulations, with respective monthly means of 2.7 ppb and 2.8 ppb for the 2019 year. Therefore, the plot shows only one curve for these

pollutants. In Figure 9, the fixed scale also means that the FEPAM values are not clearly visible. Observations are generally higher than the simulations, indicating an underestimation of emissions. Again, more suburban or regional stations, such as Pico do Jaraguá, which has wider representativity standing at the top of the mountain, show better agreement, with an average difference of 2.0 ppb. Furthermore, there is a good agreement with the remote site Amazon Tall Tower Observatory (ATTO). Nevertheless, the model is able to capture the seasonal trend for most of the stations.

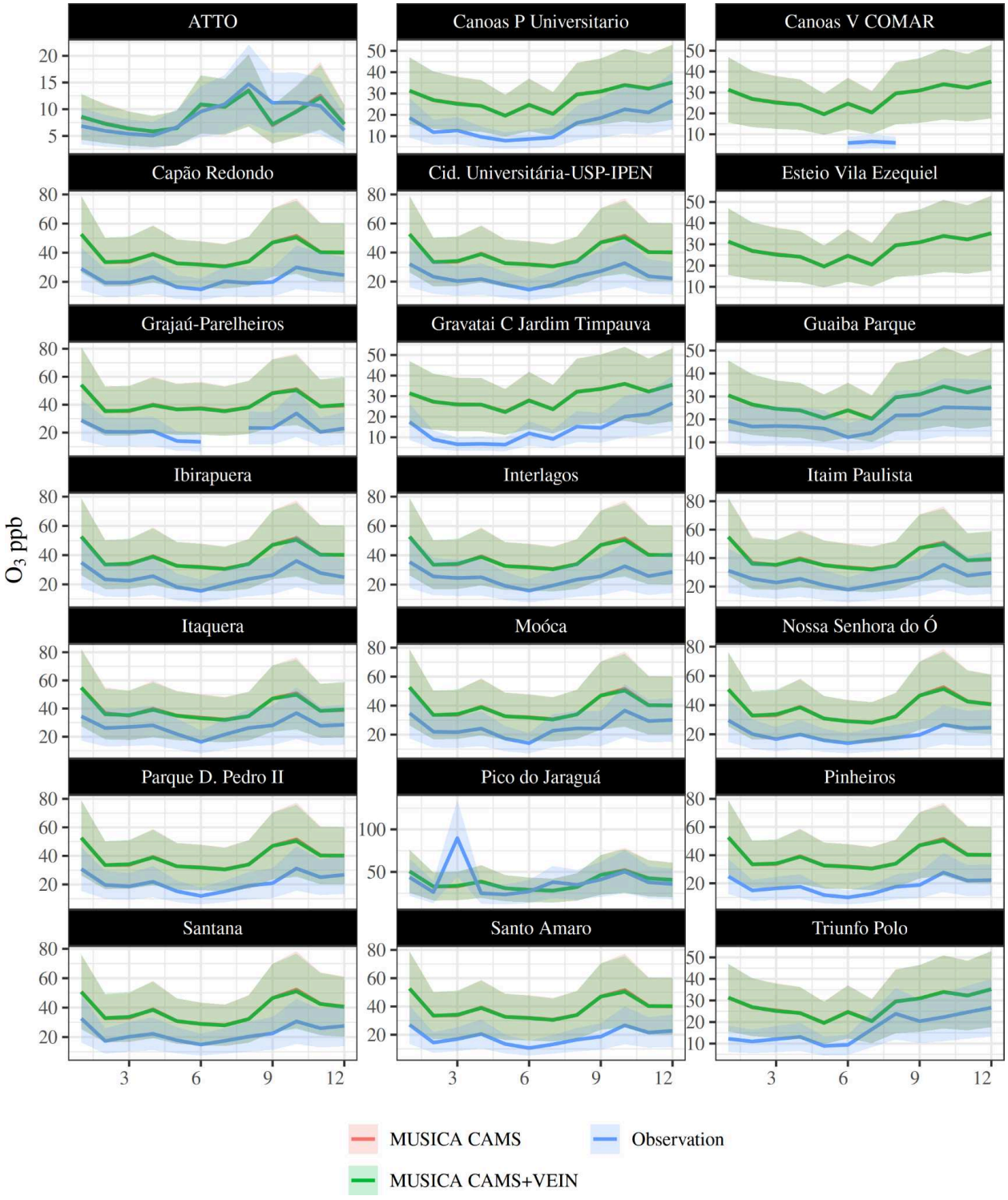
ATTO
Canoas P Universitario
Canoas V COMAR
Capão Redondo
Cid. Universitária-USP-IPEN
Esteio Vila Ezequiel
Grajaú-Parelheiros
Gravatai C Jardim Timpauva
Guaiba Parque
Ibirapuera
Interlagos
Itaim Paulista
Itaquera
Moóca
Nossa Senhora do Ó
Parque D. Pedro II
Pico do Jaraguá
Pinheiros
Santana
Santo Amaro
Triunfo Polo
O3 ppb
MUSICA CAMS
Observation
MUSICA CAMS+VEIN

Figure 9. Comparison between MUSICA CAMS, MUSICA-CAMS+VEIN, observations from the environmental protection agency in Brazil, Sao Paulo CETESB (https://cetesb.sp.gov.br/ar/), Amazon Tall Tower Observaory (ATTO, https://www.attoproject.org/) and Rio Grande do Sul (https://www.fepam.rs.gov.br/ar) as monthly mean of O_3 (ppb).

3.3.3. $PM_{2.5}$

The comparison with $PM_{2.5}$ in Brazil resulted in a really good agreement between MUSICA and observations, as shown in Figure 10. The average values for MUSICA-CAMS, MUSICA-CAMS+VEIN, and CETESB were 14.9 μg m^{-3}, 14.9 μg m^{-3}, and 16.8 μg m^{-3}, respectively. Differences between MUSICA-CAMS and MUSICA-CAMS+VEIN at the station level were on the order of one decimal place. Seasonality is also captured; however, the mid-year peak associated with the dry season is not fully reached by MUSICA. Overall, this constitutes a very good result, as it represents the first evaluation of MUSICA with surface stations in Brazil for $PM_{2.5}$.

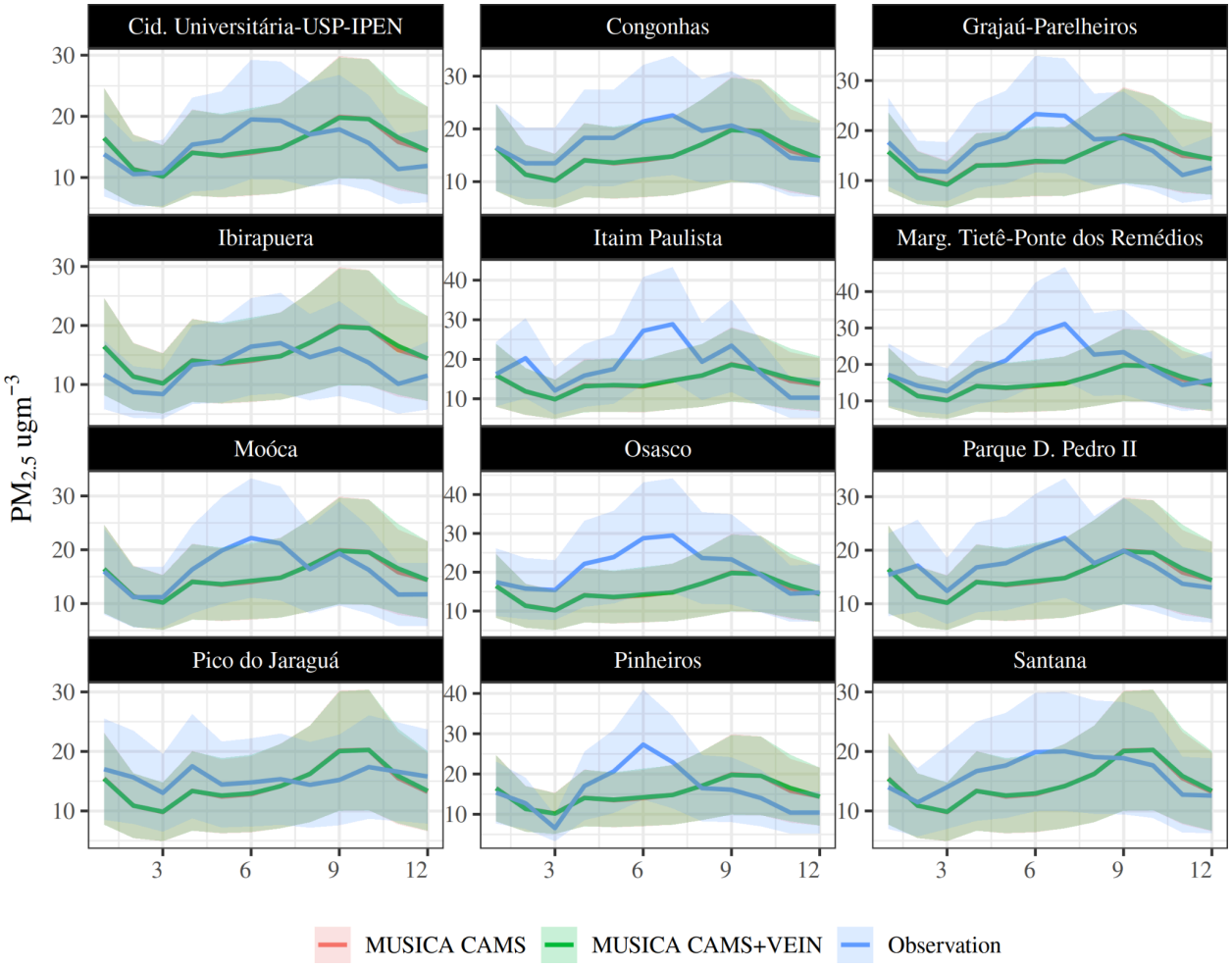

Figure 10. Comparison between MUSICA CAMS, MUSICA-CAMS+VEIN, observations from the environmental protection agency in Brazil Sao Paulo CETESB (https://cetesb.sp.gov.br/ar/) and Rio Grande do Sul (https://www.fepam.rs.gov.br/ar) as monthly mean of $PM_{2.5}$ (μg m^{-3}).

3.3.4. NO_2

The comparison for NO_2 shows that MUSICA is able to represent the seasonality of the observations, although with a smaller magnitude, as shown in Figure 11. Better agreement is found at Ibirapuera Park, followed by Interlagos. In contrast, the biggest discrepancies are found

at Marginal Tietê - Ponte dos Remédios, a street-level station, and Congonhas, a station located next to a busy airport. Interestingly, at the Pico do Jaraguá station, the model values are slightly higher than the observations. The FEPAM observations agree well with MUSICA, since it is located in an urban area smaller than Sao Paulo, near the Guaiba River (see supplementary information for location).

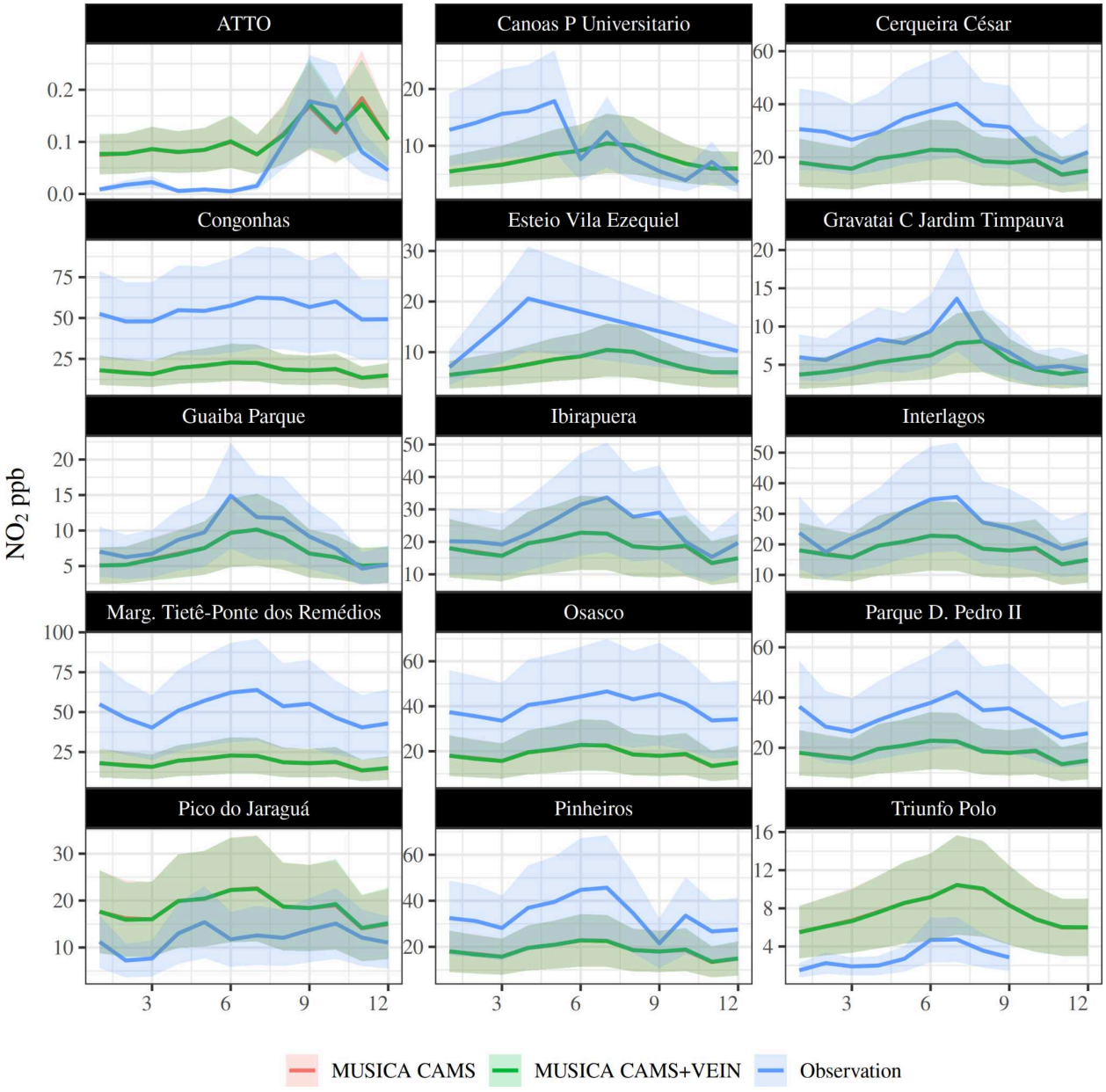

Figure 11. Comparison between MUSICA CAMS, MUSICA-CAMS+VEIN, observations from the environmental protection agency in Brazil São Paulo CETESB (https://cetesb.sp.gov.br/ar/), Amazon Tall Tower Observaory (ATTO, https://www.attoproject.org/) and Rio Grande do Sul (https://www.fepam.rs.gov.br/ar) as monthly mean of NO_2 (ppb) for 2019.

3.3.5. NO

Observed NO concentrations are generally higher than the model simulations, particularly at street-level stations, similar to the previous analysis (see Figure S31). Again, better agreement is found at the Pico do Jaraguá station. Previous WRF-CHEM simulations evaluated at the same stations also showed a negative bias for NO[50]. These results would suggest that emissions of NO (likely from traffic, industrial sources, or others) are underestimated in the model. However, a clear peak in observed NO occurs around June–August (JJA), corresponding to São Paulo's dry season. This seasonal peak is physically consistent with reduced rainfall and convective mixing leading to less vertical dispersion of pollutants, more frequent thermal inversions trapping pollutants near the surface, and more stable atmospheric layers enhancing the accumulation of primary pollutants like NO[75].

3.4. Air quality outside Brazil

The evaluation of MUSICA simulations against surface observations outside of Brazil revealed varying degrees of agreement across different countries and pollutants. Notably, stations in Chile and Colombia generally exhibited high correlation coefficients between observed and modeled pollutant concentrations, as shown in correlation Figure S31. This suggests a reasonably good performance of the modeling system in capturing the temporal dynamics of air pollutants in these regions. Furthermore, monitoring sites in Argentina (ARG) and Ecuador (ECU) also demonstrated good correlations for specific pollutants. The model performance, in terms of correlation, was strongest for O_3, followed by NO, and NO_2.

4. IMPLICATIONS

This study developed a comprehensive, long-term (1960-2100) vehicular emission inventory for Brazil, utilizing the VEIN model and localized emission factors from real-world tunnel measurements to accurately represent the region's unique biofuel and fleet composition. Applying emission factors from São Paulo to national level is a limitation. However, the southeast region in Brazil, where São Paulo is located, is the most economically powerful and, according to national statistics, contains approximately 70% of the entire national vehicle fleet[76]. That said, other regions such as rural or river dominated regions such as Amazon, may exhibit different emission and meteorological characteristics[77,78]. For instance, it is possible that in remote areas there is prevalence of poorly maintained and older fleets, leading to higher emission. Consequently, this regional extrapolation represents a source of uncertainty in our national totals, highlighting the need for future measurement campaigns in diverse Brazilian socio-economic contexts. Furthermore, currently Brazil lacks a Inspection & Maintenance program that would remove high emitter vehicles from circulation[79], implying that despite fuel-based activity and tunnel-corrected emission factors, emissions may be underestimated.

Our estimates revealed distinct historical emission patterns, with peaks for major pollutants like CO, NMHC, and $PM_{2.5}$ occurring in the 1990s and early 2000s. Crucially, comparisons with widely used global inventories (EDGAR, CEDS, CAMS) showed significant differences in the magnitude and timing of non-CO_2 pollutant peaks, highlighting the necessity of region-specific data over generalized global defaults for accurate pollutant source representation. While CO_2 emissions aligned better with global inventories due to their reliance on consistently represented

fuel consumption data, the analysis also noted the growing importance of non-exhaust particulate matter from tire, brake, and road wear in future PM projections, for which Brazil currently lacks emission control standards. A novel finding projected under different Shared Socioeconomic Pathways (SSPs) is a potential positive climate feedback mechanism where rising temperatures after approximately 2050 could increase evaporative NMHC emissions, leading to the formation of CO_2 and other greenhouse gases.

The integration of the VEIN inventory into the MUSICAv0 model for air quality simulations over Brazil, alongside global emissions elsewhere, provided an indirect evaluation of this new dataset. The model demonstrated good agreement with surface observations, particularly for $PM_{2.5}$, effectively capturing regional concentration levels and seasonal cycles. However, simply combining VEIN with CAMS emissions did not yield better agreement than CAMS alone, and limitations were observed in reproducing local-scale peaks of primary pollutants (CO, NO, NO_2) at street-level stations and during the dry season. These findings suggest a need for finer spatial resolution, improved dispersion representation, or more accurate boundary layer dynamics in the model to fully capture localized variability and the impact of atmospheric stagnation. Overall, this study delivers the first century-long, high-resolution, bottom-up vehicular emission inventory for Brazil, offering a more realistic depiction of transportation sources than previous global datasets. This improved inventory and its evaluation are vital for developing effective air quality policies, understanding historical impacts, and projecting future climate change scenarios in Brazil. Future Brazilian emission standards must specifically target the unique speciation of

exhaust, wear and evaporative emissions to prevent air quality degradation while pursuing decarbonization goals.

SUPPORTING INFORMATION

Additional details on vehicle classifications, emission factors, and fuel consumption projections; historical and future fleet data for São Paulo; state-level fuel consumption trends for ethanol, gasoline, and diesel; regional comparisons of MUSICA CAMS output with observational data from environmental agencies in South America; sensitivity analyses of fleet back-projections; and detailed descriptions of Shared Socioeconomic Pathways (SSP) in the supplement.

AUTHOR INFORMATION

Corresponding Author

*Sergio Ibarra-Espinosa sergio.ibarraespinosa@colorado.edu.

Author Contributions

The manuscript was written through contributions of all authors. All authors have given approval to the final version of the manuscript.

Funding Sources

- Part of this material is based upon work supported by the NSF National Center for Atmospheric Research, which is a major facility sponsored by the National Science Foundation under Cooperative Agreement No. 1852977.

- A. Casallas was supported by the European Union's Horizon 2020 research and innovation programme under the Marie Skłodowska-Curie grant agreement No. 101034413.
- E. D. Freitas thanks the support provided by the National Council for Scientific and Technological Development (CNPq, Process number 313210/2022-5).
- I. Silva gratefully acknowledges the financial support from the National Council for Scientific and Technological Development (CNPq), process number 140512/2021-7.
- P. Lichtig was supported by base funding from the National Commission for Atomic Energy (CNEA, Arg.) and by NSF NCAR.
- R.Y. Ynoue thanks the support provided by the National Council for Scientific and Technological Development (CNPq, Process number 406728/2022-4).
- M. A. Franco thanks the support provided by the National Council for Scientific and Technological Development (CNPq, Process number 407752/2023-4).
- G. M. Pereira thanks the support by the Fundação de Amparo à Pesquisa do Estado de São Paulo (FAPESP; Process numbers 2018/07848-9, 2016/18438-0, and 2019/01316-80) and Coordenação de Aperfeiçoamento de Pessoal de Nível Superior (CAPES; Process number 88887.103225/2025-00).
- M.F. Andrade thanks the support by FAPESP (Process number 2016/18438-0) and CNPQ (Klimapolis INCT).

Notes

Scripts available here https://github.com/ibarraespinosa/musica_vein and here https://github.com/atmoschem/vein.

ACKNOWLEDGMENT

The authors would like to acknowledge the high-performance computing support from Derecho[61] provided by NCAR's Computational and Information Systems Laboratory of the National Center for Atmospheric Research (NCAR), sponsored by the US National Science Foundation (NSF). Part of this material is based upon work supported by the National Center for Atmospheric Research, which is a major facility sponsored by the National Science Foundation under cooperative agreement no. 1852977. We also thank the computational support provided by the Departamento de Ciências Atmosféricas, Instituto de Astronomia, Geofísica e Ciências Atmosféricas, Universidade de São Paulo.

REFERENCES

1. Crippa, M.; Guizzardi, D.; Pagani, F.; Schiavina, M.; Melchiorri, M.; Pisoni, E.; Graziosi, F.; Muntean, M.; Maes, J.; Dijkstra, L.; et al. Insights into the Spatial Distribution of Global, National, and Subnational Greenhouse Gas Emissions in the Emissions Database for Global Atmospheric Research (EDGAR v8.0). Earth Syst. Sci. Data 2024, 16, 2811–2830. DOI: 10.5194/essd-16-2811-2024.
2. Rudke, A. P.; Martins, J. A.; Hallak, R.; Martins, L. D.; Almeida, D. S.; Beal, A.; Freitas, E. D.; Andrade, M. F.; Koutrakis, P.; Albuquerque, T. T. A. Evaluating TROPOMI and

MODIS Performance To Capture the Dynamic of Air Pollution in São Paulo State: A Case Study During the COVID-19 Outbreak. Remote Sens. Environ. 2023, 289, 113514.

3. Forster, P. M.; Forster, H. I.; Evans, M. J.; Gidden, M. J.; Jones, C. D.; Keller, C. A.; Lamboll, R. D.; Le Quéré, C.; Rogelj, J.; Rosen, D.; et al. Current and Future Global Climate Impacts Resulting from COVID-19. Nat. Clim. Change 2020, 10 (10), 913–919. DOI: 10.1038/s41558-020-0883-0.
4. Gaubert, B.; Bouarar, I.; Doumbia, T.; Liu, Y.; Stavrakou, T.; Deroubaix, A.; et al. Global Changes in Secondary Atmospheric Pollutants During the 2020 COVID-19 Pandemic. J. Geophys. Res.: Atmos. 2021, 126, e2020JD034213. DOI: 10.1029/2020JD034213.
5. Osses, M.; Rojas, N.; Ibarra, C.; Valdebenito, V.; Laengle, I.; Pantoja, N.; Osses, D.; Basoa, K.; Tolvett, S.; Huneeus, N.; et al. High-Resolution Spatial-Distribution Maps of Road Transport Exhaust Emissions in Chile, 1990–2020. Earth Syst. Sci. Data 2022, 14, 1359–1376. DOI: 10.5194/essd-14-1359-2022.
6. Rojas, N. Y.; Mangones, S. C.; Osses, M.; Granier, C.; Laengle, I.; Mendez, J. A. Road Transport Exhaust Emissions in Colombia. 1990–2020 Trends and Spatial Disaggregation. Transp. Res., Part D: Transp. Environ. 2023, 121, 103780.
7. CETESB. Emissões Veiculares no Estado de São Paulo, 2024. https://cetesb.sp.gov.br/veicular/relatorios-e-publicacoes/ (accessed 2024-12-16).
8. Stolf, R.; Oliveira, A. P. R. D. The Success of the Brazilian Alcohol Program (Proálcool)-a Decade-by-Decade Brief History of Ethanol in Brazil. Eng. Agríc. 2020, 40 (2), 243–248.

9. de Oliveira Gonçalves, F.; Lopes, E. S.; Lopes, M. S.; Maciel Filho, R. Thorough Evaluation of the Available Light-Duty Engine Technologies To Reduce Greenhouse Gases Emissions in Brazil. J. Cleaner Prod. 2022, 358, 132051.
10. Hoinaski, L.; Vasques, T. V.; Ribeiro, C. B.; Meotti, B. Multispecies and High-Spatiotemporal-Resolution Database of Vehicular Emissions in Brazil. Earth Syst. Sci. Data 2022, 14, 2939–2949. DOI: 10.5194/essd-14-2939-2022.
11. Ministério do Meio Ambiente (MMA). Primeiro Inventário Nacional de Emissões Atmosféricas por Veículos Automotores Rodoviários; Brasília, 2011. https://energiaeambiente.org.br/wp-content/uploads/2011/01/projeto_iema.pdf (accessed 2024-12-15).
12. Puliafito, S. E.; Bolaño-Ortiz, T. R.; Fernandez, R. P.; Berná, L. L.; Pascual-Flores, R. M.; Urquiza, J.; López-Noreña, A. I.; Tames, M. F. High-Resolution Seasonal and Decadal Inventory of Anthropogenic Gas-Phase and Particle Emissions for Argentina. Earth Syst. Sci. Data 2021, 13, 5027–5069. DOI: 10.5194/essd-13-5027-2021.
13. Romero, Y.; Chicchon, N.; Duarte, F.; Noel, J.; Ratti, C.; Nyhan, M. Quantifying and Spatial Disaggregation of Air Pollution Emissions from Ground Transportation in a Developing Country Context: Case Study for the Lima Metropolitan Area in Peru. Sci. Total Environ. 2020, 698, 134313.
14. Zalakeviciute, R.; Diaz, V.; Rybarczyk, Y. Impact of City-Wide Diesel Generator Use on Air Quality in Quito, Ecuador, During a Nationwide Electricity Crisis. Atmosphere 2024, 15 (10), 1192.

15. Zalakeviciute, R.; Lopez-Villada, J.; Ochoa, A.; Moreno, V.; Byun, A.; Proaño, E.; Mejía, D.; Bonilla-Bedoya, S.; Rybarczyk, Y.; Vallejo, F. Urban Air Pollution in the Global South: A Never-Ending Crisis? Atmosphere 2025, 16 (5), 487.
16. Vallejo, F.; Villacrés, P.; Yánez, D.; Espinoza, L.; Bodero-Poveda, E.; Díaz-Robles, L. A.; Oyaneder, M.; Campos, V.; Palmay, P.; Cordovilla-Pérez, A.; et al. Prolonged Power Outages and Air Quality: Insights from Quito's 2023–2024 Energy Crisis. Atmosphere 2025, 16 (3), 274.
17. Ibarra-Espinosa, S.; Ynoue, R. Y.; O'Sullivan, S.; Pebesma, E.; Andrade, M. D. F.; Osses, M. VEIN v0.2.2: An R Package for Bottom–Up Vehicular Emissions Inventories. Geosci. Model Dev. 2018, 11 (6), 2209–2229. DOI: 10.5194/gmd-11-2209-2018.
18. R Core Team (2024). _R: A Language and Environment for Statistical Computing_. R Foundation for Statistical Computing, Vienna, Austria. <https://www.R-project.org/>.
19. Soulie, A.; Granier, C.; Darras, S.; Zilbermann, N.; Doumbia, T.; Guevara, M.; Jalkanen, J.-P.; Keita, S.; Liousse, C.; Crippa, M.; et al. Global Anthropogenic Emissions (CAMS-GLOB-ANT) for the Copernicus Atmosphere Monitoring Service Simulations of Air Quality Forecasts and Reanalyses. Earth Syst. Sci. Data 2024, 16, 2261–2279. DOI: 10.5194/essd-16-2261-2024.
20. Pfister, G. G.; Eastham, S. D.; Arellano, A. F., Jr.; Aumont, B.; Barsanti, K. C.; Barth, M. C.; Conley, A. J.; Davis, N. A.; Emmons, L. K.; Fast, J. D.; et al. The Multi-Scale Infrastructure for Chemistry and Aerosols (MUSICA). Bull. Am. Meteorol. Soc. 2020, 101 (10), E1743–E1760. DOI: 10.1175/BAMS-D-19-0331.1.

21. Koupal, J., Beardsley, M., Brzezinski, D., Warila, J. and Faler, W., 2010. US EPA's MOVES2010 vehicle emission model: overview and considerations for international application. Ann Arbor, MI: US Environmental Protection Agency, Office of Transportation and Air Quality. https://www.epa.gov/sites/default/files/2019-08/documents/paper137-tap2010.pdf (accessed 2026-01-18).
22. Pourmatin, M., Moeini-Aghtaie, M., Hassannayebi, E. and Hewitt, E., 2024. Transition to Low-Carbon Vehicle Market: Characterization, System Dynamics Modeling, and Forecasting. Energies, 17(14), p.3525.
23. Collett, K.A., Bhagavathy, S.M. and McCulloch, M.D., 2021. Forecast of electric vehicle uptake across counties in England: Dataset from S-curve analysis. Data in Brief, 39, p.107662.
24. Kucharavy, D.; De Guio, R. Application of Logistic Growth Curve. Procedia Eng. 2015, 131, 280–290. DOI: 10.1016/j.proeng.2015.12.390.
25. Barrella, E. and Amekudzi, A.A., 2011. Backcasting for sustainable transportation planning. Transportation Research Record, 2242(1), pp.29-36.
26. Agência Nacional do Petróleo, Gás Natural e Biocombustíveis (ANP). Vendas de Derivados de Petróleo e Biocombustíveis. https://www.gov.br/anp/pt-br/centrais-de-conteudo/dados-abertos/vendas-de-derivados-de-petroleo-e-biocombustiveis (accessed 2024-12-18).
27. Bruni, A.; Bales, M. CETESB: Curvas de Intensidade de Uso por Tipo de Veículos Automotor da Frota da Cidade de São Paulo; CETESB: São Paulo, 2014.

https://repositorio.cetesb.sp.gov.br/items/c48d4a24-55cd-4fba-97c7-3cd491336bab/full (accessed 2024-12-19).

28. de Haan, P.; Keller, M. Emission Factors for Passenger Cars: Application of Instantaneous Emission Modeling. Atmos. Environ. 2000, 34 (27), 4629–4638.
29. El-Fadel, M.; Hashisho, Z. Vehicular Emissions in Roadway Tunnels: A Critical Review. Crit. Rev. Environ. Sci. Technol. 2001, 31 (2), 125–174.
30. Staehelin, J.; Keller, C.; Stahel, W. A.; Schläpfer, K.; Steinemann, U.; Buergin, T. O.; Schneider, S. Modelling Emission Factors of Road Traffic from a Tunnel Study. Environmetrics 1997, 8 (3), 219–239.
31. Martins, L. D.; Andrade, M. F.; Freitas, E. D.; Pretto, A.; Gatti, L. V.; Albuquerque, É. L.; Tomaz, E.; Guardani, M. L.; Martins, M. H.; Junior, O. M. Emission Factors for Gas-Powered Vehicles Traveling Through Road Tunnels in São Paulo, Brazil. Environ. Sci. Technol. 2006, 40 (21), 6722–6729.
32. Sánchez-Ccoyllo, O. R.; Ynoue, R. Y.; Martins, L. D.; Astolfo, R.; Miranda, R. M.; Freitas, E. D.; Borges, A. S.; Fornaro, A.; Freitas, H.; Moreira, A.; et al. Vehicular Particulate Matter Emissions in Road Tunnels in Sao Paulo, Brazil. Environ. Monit. Assess. 2009, 149, 241–249.
33. Pérez-Martínez, P. J.; Miranda, R. M.; Nogueira, T.; Guardani, M. L.; Fornaro, A.; Ynoue, R.; Andrade, M. F. Emission Factors of Air Pollutants from Vehicles Measured Inside Road Tunnels in São Paulo: Case Study Comparison. Int. J. Environ. Sci. Technol. 2014, 11, 2155–2168.

34. Nogueira, T., Kamigauti, L.Y., Pereira, G.M., Gavidia-Calderon, M.E., Ibarra-Espinosa, S., Oliveira, G.L.D., Miranda, R.M.D., Vasconcellos, P.D.C., Freitas, E.D.D. and Andrade, M.D.F., 2021. Evolution of vehicle emission factors in a megacity affected by extensive biofuel use: results of tunnel measurements in São Paulo, Brazil. Environmental Science & Technology, 55(10), pp.6677-6687.

35. Pereira, G. M.; Kamigauti, L. Y.; Nogueira, T.; Gavidia-Calderón, M. E.; Dos Santos, D. M.; Evtyugina, M.; Alves, C.; de Castro Vasconcellos, P.; Freitas, E. D.; de Fatima Andrade, M. Emission Factors for a Biofuel Impacted Fleet in South America's Largest Metropolitan Area. Environ. Pollut. 2023, 331, 121826.

36. Gavidia-Calderón, M. E.; Ibarra-Espinosa, S.; Kim, Y.; Zhang, Y.; Andrade, M. D. F. Simulation of O3 and NOx in São Paulo Street Urban Canyons with VEIN (v0.2.2) and MUNICH (v1.0). Geosci. Model Dev. 2021, 14, 3251–3268. DOI: 10.5194/gmd-14-3251-2021.

37. Grell, G. A.; Peckham, S. E.; Schmitz, R.; McKeen, S. A.; Frost, G.; Skamarock, W. C.; Eder, B. Fully Coupled “Online” Chemistry Within the WRF Model. Atmos. Environ. 2005, 39 (37), 6957–6975.

38. Kim, Y.; Wu, Y.; Seigneur, C.; Roustan, Y. Multi-Scale Modeling of Urban Air Pollution: Development and Application of a Street-in-Grid Model (v1.0) by Coupling MUNICH (v1.0) and Polair3D (v1.8.1). Geosci. Model Dev. 2018, 11, 611–629. DOI: 10.5194/gmd-11-611-2018.

39. DieselNet. Fuels: Brazil. Published 2025. https://dieselnet.com/standards/br/fuel.php (accessed Jan 4, 2025).

40. Ibarra-Espinosa, S.; Ynoue, R. Y.; Ropkins, K.; Zhang, X.; de Freitas, E. D. High Spatial and Temporal Resolution Vehicular Emissions in South-East Brazil with Traffic Data from Real-Time GPS and Travel Demand Models. Atmos. Environ. 2020, 222, 117136.
41. Instituto Nacional de Meteorologia (INMET). DADOS HISTÓRICOS ANUAIS. Ministério da Agricultura e Pecuária, 2024. https://portal.inmet.gov.br/dadoshistoricos (accessed 2024-12-28).
42. Copernicus Climate Change Service, Climate Data Store. CMIP6 Climate Projections [Data set]; Copernicus Climate Change Service (C3S) Climate Data Store (CDS), 2021. DOI: 10.24381/cds.c866074c (accessed 2024-12-28).
43. Fasola, S.; Muggeo, V. M. R.; Kuchenhoff, K. A Heuristic, Iterative Algorithm for Change-Point Detection in Abrupt Change Models. Comput. Stat. 2018, 33, 997–1015.
44. Ntziachristos, L.; Boulter, P. G. Automobile Tyre and Brake Wear and Road Abrasion. In EMEP/EEA Air Pollutant Emission Inventory Guidebook 2016; European Environment Agency: Copenhagen, Denmark, 2016.
45. Barrett, T.; Dowle, M.; Srinivasan, A.; Gorecki, J.; Chirico, M.; Hocking, T.; Schwendinger, B. data.table: Extension of data.frame; R Package Version 1.16.2; R Foundation for Statistical Computing: Vienna, Austria, 2024. https://CRAN.R-project.org/package=data.table.
46. Pebesma, E. Simple Features for R: Standardized Support for Spatial Vector Data. R J. 2018, 10 (1), 439–446. DOI: 10.32614/RJ-2018-009.
47. Pebesma, E.; Mailund, T.; Hiebert, J. Measurement Units in R. R J. 2016, 8 (2), 486–494. DOI: 10.32614/RJ-2016-061.

48. Meotti, B.; Ibarra-Espinosa, S.; Hoinaski, L. Improving Spatial Disaggregation of Vehicular Emission Inventories. Environ. Technol. 2025, 1–14.

49. OpenStreetMap contributors. OpenStreetMap Data Extracts. Geofabrik GmbH. Published 2023. https://download.geofabrik.de/ (accessed 2024-12-2028).

50. Ibarra-Espinosa, S.; da Silva, G. A. M.; Rehbein, A.; Vara-Vela, A.; de Freitas, E. D. Atmospheric Effects of Air Pollution During Dry and Wet Periods in São Paulo. Environ. Sci.: Atmos. 2022, 2 (2), 215–229.

51. Carter, W. P. Development of a Database for Chemical Mechanism Assignments for Volatile Organic Emissions. J. Air Waste Manage. Assoc. 2015, 65 (10), 1171–1184.

52. Crippa, M.; Guizzardi, D.; Pisoni, E.; Solazzo, E.; Guion, A.; Muntean, M.; Florczyk, A.; Schiavina, M.; Melchiorri, M.; Hutfilter, A. F. Global Anthropogenic Emissions in Urban Areas: Patterns, Trends, and Challenges. Environ. Res. Lett. 2021, 16 (7), 074033.

53. McDuffie, E. E.; Smith, S. J.; O'Rourke, P.; Tibrewal, K.; Venkataraman, C.; Marais, E. A.; Zheng, B.; Crippa, M.; Brauer, M.; Martin, R. V. A Global Anthropogenic Emission Inventory of Atmospheric Pollutants from Sector- and Fuel-Specific Sources (1970–2017): An Application of the Community Emissions Data System (CEDS). Earth Syst. Sci. Data 2020, 12, 3413–3442. DOI: 10.5194/essd-12-3413-2020.

54. Lichtig, P.; Gaubert, B.; Emmons, L. K.; Jo, D. S.; Callaghan, P.; Ibarra‐Espinosa, S.; Dawidowski, L.; Brasseur, G. P.; Pfister, G. Multiscale CO Budget Estimates Across South America: Quantifying Local Sources and Long Range Transport. J. Geophys. Res.: Atmos. 2024, 129 (8), e2023JD040434. DOI: 10.1029/2023JD040434.

55. Emmons, L. K.; Schwantes, R. H.; Orlando, J. J.; Tyndall, G.; Kinnison, D.; Lamarque, J.-F.; et al. The Chemistry Mechanism in the Community Earth System Model Version 2 (CESM2). J. Adv. Model. Earth Syst. 2020, 12, e2019MS001882. DOI: 10.1029/2019MS001882.

56. Liu, X.; Ma, P.-L.; Wang, H.; Tilmes, S.; Singh, B.; Easter, R. C.; Ghan, S. J.; Rasch, P. J. Description and Evaluation of a New Four-Mode Version of the Modal Aerosol Module (MAM4) Within Version 5.3 of the Community Atmosphere Model. Geosci. Model Dev. 2016, 9, 505–522. DOI: 10.5194/gmd-9-505-2016.

57. Tilmes, S.; Hodzic, A.; Emmons, L. K.; Mills, M. J.; Gettelman, A.; Kinnison, D. E.; et al. Climate Forcing and Trends of Organic Aerosols in the Community Earth System Model (CESM2). J. Adv. Model. Earth Syst. 2019, 11, 4323–4351. DOI: 10.1029/2019MS001827.

58. Gelaro, R.; McCarty, W.; Suárez, M. J.; Todling, R.; Molod, A.; Takacs, L.; Randles, C. A.; Darmenov, A.; Bosilovich, M. G.; Reichle, R.; et al. The Modern-Era Retrospective Analysis for Research and Applications, Version 2 (MERRA-2). J. Clim. 2017, 30 (14), 5419–5454. DOI: 10.1175/JCLI-D-16-0758.1.

59. Wiedinmyer, C.; Kimura, Y.; McDonald-Buller, E. C.; Emmons, L. K.; Buchholz, R. R.; Tang, W.; Seto, K.; Joseph, M. B.; Barsanti, K. C.; Carlton, A. G.; et al. The Fire Inventory from NCAR Version 2.5: An Updated Global Fire Emissions Model for Climate and Chemistry Applications. Geosci. Model Dev. 2023, 16 (13), 3873–3891.

60. Guenther, A. B.; Jiang, X.; Heald, C. L.; Sakulyanontvittaya, T.; Duhl, T.; Emmons, L. K.; Wang, X. The Model of Emissions of Gases and Aerosols from Nature Version 2.1

(MEGAN2.1): An Extended and Updated Framework for Modeling Biogenic Emissions. Geosci. Model Dev. 2012, 5, 1471–1492. DOI: 10.5194/gmd-5-1471-2012.

61. Computational and Information Systems Laboratory CISL. 2023. Derecho: HPE Cray EX System (NCAR Community Computing). Boulder, CO: National Center for Atmospheric Research. doi:10.5065/qx9a-pg09.
62. Catalán, F.; Chandia, D.; Toro Araya, R.; Leiva Guzman, M. A. The AtmChile Open-Source Interactive Application for Exploring Air Quality and Meteorological Data in Chile. Atmosphere 2022, 13 (9), 1364.
63. Gavidia-Calderón, M.; Schuch, D.; Andrade, M. d. F. qualR: An R Package to Download Sao Paulo and Rio de Janeiro Air Pollution Data; 2022. https://docs.ropensci.org/qualR/.
64. Gavidia-Calderón, M. limaair: Download Air Quality Data from Lima Peru; R Package Version 0.0.0.9000; 2025. https://github.com/quishqa/limaair.
65. Vallejo, F. AirEcuador: Extracción y Análisis de Datos Ambientales de Quito; R Package Version 0.1.0; 2025. https://github.com/fvallejog/AirEcuador.
66. IDEAM. SISAIRE: Air Quality in Colombia, 2023. http://sisaire.ideam.gov.co/ideam-sisaire-web/informacion.xhtml?de=que_es (accessed Dec 28, 2024).
67. Casallas, A.; Cabrera, A.; Guevara-Luna, M. A.; Tompkins, A.; González, Y.; Aranda, J.; Belalcazar, L. C.; Mogollon-Sotelo, C.; Celis, N.; Lopez-Barrera, E.; et al. Air Pollution Analysis in Northwestern South America: A New Lagrangian Framework. Sci. Total Environ. 2024, 906, 167350.

68. Hoesly, R.; Smith, S. J.; Prime, N.; Ahsan, H.; Suchyta, H.; O'Rourke, P.; Crippa, M.; Klimont, Z.; Guizzardi, D.; Behrendt, J.; et al. CEDS v_2024_07_08 Release Emission Data (v_2024_07_08) [Data set]; Zenodo, 2024. DOI: 10.5281/zenodo.12803197.

69. Christou, A., Giechaskiel, B., Olofsson, U., & Grigoratos, T. (2025). Review of Health Effects of Automotive Brake and Tyre Wear Particles. Toxics, 13(4), 301. https://doi.org/10.3390/toxics13040301

70. Schuch, D. eva3dm: A R-Package for Model Evaluation of 3D Weather and Air Quality Models. J. Open Source Softw. 2025, 10 (108), Paper 7797.

71. Pachón, J. E.; Opazo, M. A.; Lichtig, P.; Huneeus, N.; Bouarar, I.; Brasseur, G.; Li, C. W. Y.; Flemming, J.; Menut, L.; Menares, C.; et al. Air Quality Modeling Intercomparison and Multiscale Ensemble Chain for Latin America. Geosci. Model Dev. 2024, 17, 7467–7512. DOI: 10.5194/gmd-17-7467-2024.

72. González, C. M.; Gómez, C. D.; Rojas, N. Y.; Acevedo, H.; Aristizábal, B. H. Relative Impact of On-Road Vehicular and Point-Source Industrial Emissions of Air Pollutants in a Medium-Sized Andean City. Atmos. Environ. 2017, 152, 279–289.

73. Huneeus, N.; van Der Gon, H. D.; Castesana, P.; Menares, C.; Granier, C.; Granier, L.; Alonso, M.; de Fatima Andrade, M.; Dawidowski, L.; Gallardo, L.; et al. Evaluation of Anthropogenic Air Pollutant Emission Inventories for South America at National and City Scale. Atmos. Environ. 2020, 235, 117606.

74. Antezana Lopez, F. P.; Casallas, A.; Zhou, G.; Zhang, K.; Jing, G.; Ali, A.; Lopez-Barrera, E.; Belalcazar, L. C.; Rojas, N.; Jiang, H. High-Resolution Anthropogenic

Emission Inventories with Deep Learning in Northern South America. Remote Sens. Environ. 2025, 324, 114761. DOI: 10.1016/j.rse.2025.114761.

75. Saide, P.E., Carmichael, G.R., Spak, S.N., Gallardo, L., Osses, A.E., Mena-Carrasco, M.A. and Pagowski, M., 2011. Forecasting urban PM10 and PM2. 5 pollution episodes in very stable nocturnal conditions and complex terrain using WRF–Chem CO tracer model. Atmospheric Environment, 45(16), pp.2769-2780.
76. Gavidia-Calderón, M.; et al. Air Quality Modeling in the Metropolitan Area of São Paulo, Brazil: A Review. Atmos. Environ. 2023, Article 120301.
77. D'Oliveira, F.A., Dias-Júnior, C.Q., Cohen, J.C., Spracklen, D.V., Marques Filho, E.P. and Artaxo, P., 2023. Effects of the river breeze on the transport of gases in Central Amazonia. Atmospheric Research, 295, p.107010.
78. Mantovani Júnior, J.A., Aravéquia, J.A., Carneiro, R.G. and Fisch, G., 2023. Evaluation of PBL parameterization schemes in WRF model predictions during the dry season of the central Amazon Basin. Atmosphere, 14(5), p.850.
79. Ibarra-Espinosa, S., Mera, Z., Ropkins, K., & Mantovani Junior, J. A. (2026). Quantifying the Impact of High Emitters on Vehicle Emissions: An Analysis of Ecuador's Inspection and Maintenance Program. Atmosphere, 17(1), 31. https://doi.org/10.3390/atmos17010031